

**THE EFFECTS OF DIABATIC HEATING ON UPPER-
TROPOSPHERIC ANTICYCLOGENESIS**

by

Ross A. Lazear

A thesis submitted in partial fulfillment of
the requirements for the degree of

Master of Science

(Atmospheric and Oceanic Sciences)

at the

UNIVERSITY OF WISCONSIN - MADISON

2007

Abstract

The role of diabatic heating in the development and maintenance of *persistent*, upper-tropospheric, large-scale anticyclonic anomalies in the subtropics (subtropical gyres) and middle latitudes (blocking highs) is investigated from the perspective of potential vorticity (PV) non-conservation. The low PV within blocking anticyclones is related to condensational heating within strengthening upstream synoptic-scale systems. Additionally, the associated convective outflow from tropical cyclones (TCs) is shown to build upper-tropospheric, subtropical anticyclones. Not only do both of these large-scale flow phenomena have an impact on the structure and dynamics of neighboring weather systems, and consequently the day-to-day weather, the very persistence of these anticyclones means that they have a profound influence on the seasonal climate of the regions in which they exist.

A blocking index based on the meridional reversal of potential temperature on the dynamic tropopause is used to identify cases of wintertime blocking in the North Atlantic from 2000-2007. Two specific cases of blocking are analyzed, one event from February 1983, and another identified using the index, from January 2007. Parallel numerical simulations of these blocking events, differing only in one simulation's neglect of the effects of latent heating of condensation (a "fake dry" run), illustrate the importance of latent heating in the amplification and wave-breaking of both blocking events. Anticyclogenesis in the "fake dry" runs is shown to be weaker than in the full physics simulations. Additionally, adjoint sensitivity studies were performed on the January 2007 blocking case with a response function specified as the low values of upper-tropospheric PV within the block. Results show that the low PV is sensitive to the strength of the upstream upper trough, as well as a

region where an explosive cyclogenesis event (and thus, large amounts of latent heating) was taking place.

The significant latent heating within the circulation of a strong TC also alters the upper-tropospheric circulation through PV redistribution, creating a broad, upper-tropospheric, anticyclonic circulation. A case study of these “outflow footprints” of Atlantic hurricanes Ophelia and Rita (2005) is presented. Specifically, the development of Ophelia’s outflow circulation and its effects on the development of Hurricane Rita are discussed. Unlike with blocking events, TC outflow anticyclones *cannot* be maintained adiabatically. The TC anticyclone, if removed from the westerlies and not supported diabatically by the TC convection, slowly decays while persisting for several days.

Acknowledgements

My first thanks go to Dr. Michael Morgan, who I am very grateful to have had as an advisor. Throughout my time as an undergraduate and graduate student at AOS, Michael was always available and willing to help, whether it was for simple programming questions, or complex, scientific issues. I also value my friendship with Michael, whose animated, boisterous behavior while at long lunches, dinners and research group parties were always entertaining, and certainly took away some of the stress of academics. Also, without Michael, the word “concomitant” would definitely be absent from this thesis.

Next, my thanks go out to the entire AOS department faculty. Specifically, I’d like to acknowledge Dr. Jon Martin and Dr. John Young for their interesting discussions and valuable suggestions after reading this thesis. Furthermore, after years of needing computer assistance or data acquisition, I’m fairly certain that Pete Pokrandt is the greatest systems administrator in the world.

I’d also like to thank my close friends and acquaintances in the AOS department. In the “Morgan research group,” Nick Bassill, for office and lab camaraderie and for accompanying me “chasing” Hurricane Katrina on the Mississippi coast; Brett Hoover for creating rap music out of the NOGAPS adjoint code with me; Dianna Nelson for bringing Ertel and Ekman to the lab; Li Bi for being a great office-mate and for buying us all lots of candy in Monterey; Dan Chavas, who I can clearly hear laugh from anywhere in the AOS building, and Andy Hulme, for being the honorary “Morgan groupie” and a good roommate.

Finally, I’d like to acknowledge my family. I would never have gotten this far without the love, support and encouragement from my parents, Jonathon and Wendy. As a weather-obsessed child, my parents fueled my interest in the subject by agreeing to wake me

up in the middle of the night if there was any interesting severe weather approaching the Twin Cities (without which, I would have likely never slept!). I would also like to thank my parents and my brother, Mike, for always reminding me how worthwhile it has been (and will be) to follow my passion.

This research was supported by the National Science Foundation with funds from Grant ATM-0121186.

Table of Contents

Abstract	i
Acknowledgements.....	iii
1. Introduction	
a. Northern Hemispheric low frequency variability	1
b. Persistent large-scale cyclones (extended jet)	3
c. Persistent large-scale anticyclones (blocking).....	4
2. The effect of latent heating on the formation of atmospheric blocking	
2.1 Introduction.....	12
2.2 Data and blocking case retrieval methodology	
a. Data sets.....	18
b. Blocking indices in recent research	18
c. Blocking event identification.....	20
d. North Atlantic blocking events.....	24
2.3 Case studies.....	25
a. February 1983 case	27
b. January 2007 case	35
2.4 Moist vs. dry simulations.....	43
2.5 Adjoint sensitivity study	
a. Introduction.....	49
b. Adjoint modeling system	50
c. Sensitivities of R_1 to vorticity	53
d. Sensitivities of R_2 to vorticity.....	55

e. Sensitivities of R_3 to vorticity	56
f. Discussion	57
2.6 Conclusion.....	58
3. The influence of tropical cyclone outflow on the upper-tropospheric circulation	
3.1 Introduction.....	62
3.2 Case study	
a. Data	64
b. Synoptic overview	64
3.3 Discussion and future work.....	69
4. Conclusions.....	71

1. Introduction

a. Northern Hemispheric low frequency variability

The seasonally averaged mid-latitude circulation is characterized by planetary-scale waves that are forced by large-scale topographic features, diabatic heating, and transient eddy fluxes of (potential) vorticity. Spectral model simulations with realistic land/sea geography and topography show storm track regions east of large topographic features, such as over the western North Pacific and east of North America over the North Atlantic (Wallace and Lau 1985). Downstream of these storm tracks are local maxima in low-pass filtered temporal root mean square of 500-hPa height, owing to the fact that these regions are dominated by *low*-frequency variability (often defined as planetary-scale waves with periods greater than 10 days). In these simulations, scale interactions are also evident, with upstream high frequency eddies acting to transport momentum into the storm track regions, thus enhancing and maintaining the longwave pattern. Using simple linear models, Derome and Wiin-Nielsen (1971) and Lin (1982) showed that diabatic heating makes a strong contribution to the development and maintenance of planetary-scale waves. This process will be thoroughly discussed in this paper, specifically concerning the dynamics of the development of large-scale anticyclonic anomalies through diabatic heating.

In order to locate dominant modes of low-frequency variability in the mid-latitudes and understand the processes by which these modes develop, Blackmon (1976) separated 500-hPa geopotential height data into three separate wavenumber regimes. He showed that planetary-scale contributions to the total wintertime variability over a 9-year period are mainly confined to high latitudes and over mid-latitude oceans. Blackmon et al. (1977) showed that low-pass filtered (between 10 and 90 days) geopotential height variability is

essentially barotropic, and that the maximum variance in low-pass filtered geopotential height appears downstream of the major mid-latitude storm tracks. Wallace and Gutzler (1981) described the structure of dominant regional patterns of low-frequency variability in the mid-tropospheric geopotential height fields (teleconnection patterns), such as the Pacific-North American (PNA) pattern and the North Atlantic Oscillation (or NAO, which was originally identified by Walker and Bliss 1932). The PNA and NAO are the dominant modes of low-frequency variability in the Pacific and Atlantic basins, respectively. In a barotropic stability analysis of the climatological winter-time (December, January and February) mean flow, Simmons et al. (1983) showed that the PNA and NAO patterns of low-frequency variability resemble the normal modes of the DJF time-mean flow.

A positive NAO index is associated with a strong Icelandic low and enhanced westerlies across the North Atlantic while a negative index is associated with an anomalous anticyclone in the North Atlantic and a concomitant decrease in westerlies to its south. Positive (negative) values of the PNA index are associated with a deep Aleutian low (anomalous central Pacific anticyclone) and downstream ridge (trough), with negative (positive) upper-tropospheric height anomalies over the southeastern United States. The PNA and NAO patterns are associated with significant sensible weather over North America and Europe, respectively.

Charney and DeVore (1979) studied the effect of external forcing on planetary-scale motions. Using a barotropic spectral model, the authors showed that multiple equilibrium states can exist for perturbations forced by topography, or by thermal asymmetries in the flow. In this case, flows that interact with topography or thermal asymmetries appear to lock to a nearly resonant state. Two types of equilibrium states appear to be associated with

topographic forcing, flow with a high amplitude wave which is zonally weak, and one with a strong zonal component. Those equilibrium flows with high amplitude waves are said to appear “blocked,” and have a strongly meridional flow. The equilibrium state with the strong zonal component has an intense, extended jet. The model used by Charney and DeVore (1979) showed that high amplitude ridges (blocks) appear west of large topographic features, which tends to correspond well with the preferred regions of blocking in the North Hemisphere. The state of the system in their model appears to oscillate from one steady state to another through small-scale instabilities. Hanson and Sutera (1995) showed that there is a positive correlation between the variance of low-frequency variability and the height of the continental topography. Decreased height of topographical features results in an increase in high-frequency variance, but a decrease in low-frequency variance, thus showing the importance of topography in determining the location of dominant modes of low-frequency variability.

b. Persistent large-scale cyclones (extended jet)

There have been numerous studies on the structure and formation of persistent large-scale cyclonic anomalies. Dole and Gordon (1983) showed that low-pass filtered large-scale cyclone cases (i.e., 500-hPa height anomalies less than -100 m lasting 10 or more days) are generally confined to the North Pacific and North Atlantic. Black and Dole (1993) found that large-scale cyclogenesis events over the North Pacific are correlated with the PNA pattern, and associated with an anomalously strong and eastward-extending zonal jet over the North Pacific. High upper-tropospheric PV over eastern Asia becomes advected east in association with a developing surface cyclone. The entire system acquires an equivalent

barotropic structure and becomes nearly stationary over the North Pacific. Through the use of an adjoint sensitivity study, Keller et al. (2006) showed that, for a particular case of large-scale cyclogenesis, sensitivities are maximized in regions of barotropic and baroclinic shear 48 hours prior to event onset. This suggests that the development of this specific persistent cyclone is driven by mid-latitude baroclinic and barotropic processes, rather than anomalous tropical heating.

c. Persistent large-scale anticyclones (blocking)

Blocked atmospheric flow is associated with a split, upper-tropospheric westerly jet, marked by significant meridional excursions in the upper-tropospheric, mid-latitude flow in the regions surrounding the block. Weather systems are restricted from progressing through the blocked region and are consequently averted around a blocking anticyclone. Following the model used by Charney and DeVore (1979), Northern Hemisphere blocking events are generally favored over the northeast Pacific and northeast Atlantic/Europe (Rex 1950; Lejenäs and Økland 1983).

Blocking patterns have been shown to have prolonged, dramatic effects on the sensible weather in their vicinity. Typically, relatively warm and dry weather exists beneath a blocking anticyclone, where large positive upper-tropospheric height anomalies are located. To the south, a cut-off upper-tropospheric low often occurs (dipole blocks), which is associated with a prolonged period of cool and wet weather (Rex 1950; 1951; Pettersen, 1956). Quiroz (1984) showed that the anomalously cold winter of 1983-84 over the central and western United States was the result of frequent blocking episodes over the northeast Pacific.

In addition to the long-duration, anomalous weather that accompanies a blocking event, there are numerous predictability issues associated with the onset and duration of blocking. Tibaldi and Molteni (1990, hereafter TM90) and Pelly and Hoskins (2003) found that the European Centre for Medium-Range Weather Forecasts (ECMWF)'s operational model forecasts a much slower transition to blocking than what is observed. Additionally, in the ECMWF model, blocking frequency is dramatically underforecast, especially in the medium range (TM90). Furthermore, TM90 found that most medium-range forecast models underestimate the duration of blocking events, though this aspect of the forecast is handled better by numerical models than the prediction of the block onset itself. Pelly and Hoskins (2003) also showed that the onset of a blocking event is typically more difficult to predict than its decay, and speculated that this is due to the inherent differences in the dynamics of blocking onset and decay. It was proposed that the difficulty in predicting block onset is due to the fact that a block's onset is dependent on rapidly developing synoptic-scale disturbances. Block decay, however, is often a more gradual process, as it is associated with processes that have a longer time-scale, such as radiative cooling.

Colucci (2001) examined precursors of atmospheric blocking events and showed that many models poorly forecast a block's precursor diffluent jet. Tracton (1990) showed that low resolution, spectral (rhomboidal R40) medium range forecasts generated by the National Meteorological Center completely failed in developing a block more than three days in advance. However, with a finer spectral resolution (triangular T80), the predictability of block onset improves dramatically. Lupo and Smith (1998) showed that the rapid 500-hPa geopotential height rise during block development is more of a synoptic-scale (and interaction between synoptic- and planetary-scale) process than a planetary-scale process.

These factors point to the fact that synoptic-scale processes are integral for the onset of a blocking event.

Colucci (2001) showed that the upper-tropospheric flow antecedent to blocking is characterized by negative planetary-scale geostrophic stretching deformation. Using a nonlinear barotropic vorticity model forced with a wavemaker and simple Ekman damping, Shutts (1983; 1986) deduced the role of eddy forcing on the creation of a blocking anticyclone. It was shown that strong anticyclonic vorticity forcing (eddy vorticity flux divergence) was prevalent approximately two days prior to block onset. Illari (1984) showed that this upstream eddy forcing is necessary in maintaining the blocking high and preventing the pattern from moving downstream. Additionally, Shutts (1983) discovered that with the presence of a strong deformation field within a pre-existing jet, an enhanced momentum flux into the block occurs as synoptic-scale eddies become zonally compressed and meridionally elongated. This eddy straining process appears to be a self-maintaining mechanism which enables the blocking anticyclone to sustain itself for a long duration (Shutts 1986; Mak 1991).

In order to further investigate the dynamics of synoptic-scale processes in the onset and maintenance of a blocking anticyclone, potential vorticity (PV), as well as isentropic analyses (Morgan and Nielsen-Gammon 1998) have been examined (Illari 1984; Morgan et al. 1991; Lackmann et al. 1996; Colucci 2001; Schwierz et al. 2004; Dong and Colucci 2005). Illari (1984) demonstrated that low values of upper-tropospheric PV are advected poleward from the tropics into the block. These results corroborate those of Mahlman (1979) and Nakamura and Wallace (1993) which showed that rapid intensification of a blocking anticyclone occurs when an anticyclonic eddy advects low PV air into the western flank of

the block from low to mid latitudes. Dong and Colucci (2005) explained that, in the Southern Hemisphere, equatorward increasing cyclonic PV within a diffluent flow forces a weakening of geostrophic westerlies, thus aiding in the production of a blocking anticyclone.

A number of studies have shown a connection between explosive cyclogenesis and the downstream genesis of a blocking anticyclone. Nakamura and Wallace (1990; 1993) depicted an enhanced region of baroclinic wave activity in upstream storm track regions approximately 5 days before block onset. Konrad and Colucci (1988) showed a large correlation between 500-hPa block-like patterns and nearby explosive cyclogenesis events. The authors hypothesized that the critical condition for the onset of blocking may be the long duration, meridional transport of air parcels immediately following surface cyclogenesis. Additionally, Alberta et al. (1991) showed that a case of pre-blocking rapid upper-tropospheric anticyclonogenesis is preceded by “nearly rapid” surface cyclogenesis upstream.

Lackmann et al. (1996) analyzed a 6-day composite of 42 rapidly deepening cyclones over the western North Atlantic in order to study the synoptic and planetary scale environment associated with explosive cyclogenesis. The authors showed that the wavelength between the amplifying trough and downstream ridge associated with rapid cyclogenesis decreases significantly. This characteristic of explosive cyclogenesis events helps to enhance the meridional component of the flow, which increases the likelihood for a blocking event to occur, simply by advecting low PV poleward from the subtropics. In a 30-year composite of blocking events, Nakamura and Wallace (1993) showed that an intense surface cyclone helps advect low PV poleward downstream, which helps to amplify the blocking anticyclone. It was shown that two distinct synoptic-scale systems advect low PV from low latitudes into the developing ridge: one approximately a day prior to block onset,

and one two days following block onset. These results are consistent with a number of studies (Crum and Stevens 1988; Illari 1984; Nakamura et al. 1997), which showed that much of the low PV found within the anticyclonic portion of a block originated at low latitudes.

Though the majority of research on atmospheric blocking has focused primarily on *adiabatic*, dynamical mechanisms such as scale interactions, (potential) vorticity fluxes, and the effect of synoptic-scale eddies on forming and maintaining a block, one important aspect of block onset and maintenance that has been somewhat overlooked is the role of moist, thermodynamic processes, namely latent heating. There is evidence that diabatic heating may play an important role in the development (and maintenance) of blocking events. As previously stated, studies such as that of Konrad and Colucci (1988) have linked processes associated with rapidly deepening cyclones with the onset of a blocking event downstream. In addition, though some of the low PV within a blocking anticyclone has subtropical origins, it appears likely that the lens of low upper-tropospheric PV within a block may have its origins from PV redistributed through latent heating within the ascent region of an upstream cyclone.

In the Northern Hemisphere, diabatic heating in the mid-troposphere redistributes PV by diminishing the PV aloft and redistributing it to the lower troposphere. It has been shown that 40-50% of the deepening during explosive cyclogenesis occurs through latent heating (Reed et al. 1988). This process would likely facilitate amplification of an upper-tropospheric ridge downstream from an explosively deepening cyclone through upper-tropospheric PV reduction. Thus, since atmospheric blocking tends to follow rapid cyclogenesis events (Konrad and Colucci 1988), it may be expected that it is the latent

heating associated with the deepening cyclone which causes the lowering of the upper-tropospheric PV downstream, ultimately leading to a blocking event. In fact, Mahlman (1979) noted that there appears to be especially low upper-tropospheric PV on the western flank of a blocking anticyclone. The location of this anomalously low upper-tropospheric PV would tend to be collocated with the latent heat release of an upstream deepening cyclone, potentially supporting the hypothesis that latent heating aids in the production of a blocking anticyclone.

Prior research on the effects of diabatic heating on block development supports this hypothesis. In a trajectory analysis of a case of North Atlantic blocking, Crum and Stevens (1988) showed that latent heating dramatically affected the trajectories of air parcels as they moved into the anticyclonic region of the block. In a simulation of this blocking case, air parcels experiencing condensation acquired a much more amplified anticyclonic circulation and moved poleward more than parcels without latent heating. Due to the importance of latent heating as well as advection of low PV from low latitudes east of a strong cyclone, it was concluded that developing cyclones may play an important role in block development. Recent research by Schwierz (2001) has also shown that the low PV (<1 PVU) within a blocking anticyclone is partially attributed to latent heating. In an analysis of a North Atlantic blocking case from January 1987, Schwierz (2001) showed that 80% ($>20\%$) of 72-hr trajectories ending within the blocking anticyclone are cross-isentropic with a change in potential temperature of more than 5 K (20 K). Also of note is that for this specific case of blocking, less than 20% of trajectories ending within the blocked region of $PV < 0.5$ originated in the tropics. Thus, it was shown that the development of the January 1987 blocking case was almost entirely diabatically forced.

In summary, much of the research on block development has been focused solely on adiabatic, dynamical processes. Strong anticyclonic vorticity fluxes occur approximately two days prior to block onset, and this forcing is also necessary in maintaining the block and preventing its downstream movement. From a PV perspective, it has been shown that low upper-tropospheric PV found within a blocking anticyclone is advected poleward from low latitudes (Illari 1984), often aided by advection downstream of a rapidly developing cyclone (Konrad and Colucci 1988). Additionally, Nakamura and Wallace (1990) showed that there is enhanced upstream baroclinic wave activity approximately 5 days prior to block onset. There is, however, some evidence which points to PV redistribution associated with diabatic heating as the origin of the low PV within the anticyclonic portion of a block. Trajectory analyses for specific blocking cases (Crum and Stevens 1988; Schwierz 2001) have shown that condensational heating played a major role in the development of a block. During cyclogenesis, PV is redistributed such that the upper-tropospheric PV (Northern Hemisphere) diminishes on the western flank of a developing ridge, which ultimately forces a stronger anticyclonic circulation, and thus, a more amplified ridge. Additionally, in a case study of a major blocking event in 1983, Morgan et al. (1991) attributed the block's initial development to latent heating along an intense squall line and the maintenance of the block to latent heating in multiple subsequent cyclogenesis events.

This thesis describes the contribution of diabatic heating within synoptic and mesoscale weather systems to low frequency variability defined on times scales of a week or more. Chapter 2 of this thesis focuses on the effects of diabatic heating on the formation and maintenance of atmospheric blocking, and is written to stand alone as a paper to be peer-reviewed. In this chapter, a blocking index similar to that described by Pelly and Hoskins

(2003) is applied to gridded atmospheric analyses. Particular blocking cases identified by this index are then diagnosed using the gridded analyses, model simulations, and adjoint sensitivity studies. Chapter 3 describes the effects of diabatic heating in a tropical cyclone on the upper troposphere subtropical circulation. This work was previously presented at the 27th AMS Conference on Hurricanes and Tropical Meteorology. A summary of the thesis work, as well as a description of possible future work on this subject, is presented in Chapter 4.

Chapter 2. The effect of latent heating on the formation of atmospheric blocking

2.1 Introduction

Atmospheric blocking is a phenomenon characterized by the impedance (or blocking) of the typical west to east progression of transient mid-latitude weather systems by a large-amplitude, large-scale anticyclone (Namias and Clapp 1944; Elliot and Smith 1949; and Rex 1950; 1951). The life-cycle of a blocking anticyclone is much longer than the life-cycle of the transient weather systems whose eastward progression the block thwarts. Using 500-hPa geopotential height analyses, Rex (1950; 1951) established one of the first subjective definitions for blocks:

- (i) there must be a jet split that abruptly changes the flow from predominantly westerly to predominantly meridional;
- (ii) the jet split must extend at least 45° longitude;
- (iii) each jet east of the split must transport substantial mass; and
- (iv) the pattern must persist for a minimum of ten days.

An example of a major North Atlantic blocking event from 22 January – 2 February 2007 which will be analyzed in detail in this paper is shown in Fig. 1, using $1^\circ \times 1^\circ$ NCEP/NCAR final analysis data. Fig. 2.1a depicts the 300-hPa geopotential height and absolute vorticity fields during the middle of the blocking event (1200 UTC 26 January 2007), which satisfies each of the criteria above. A large upper-tropospheric anticyclonic circulation with relatively uniform absolute vorticity was positioned from Greenland to the

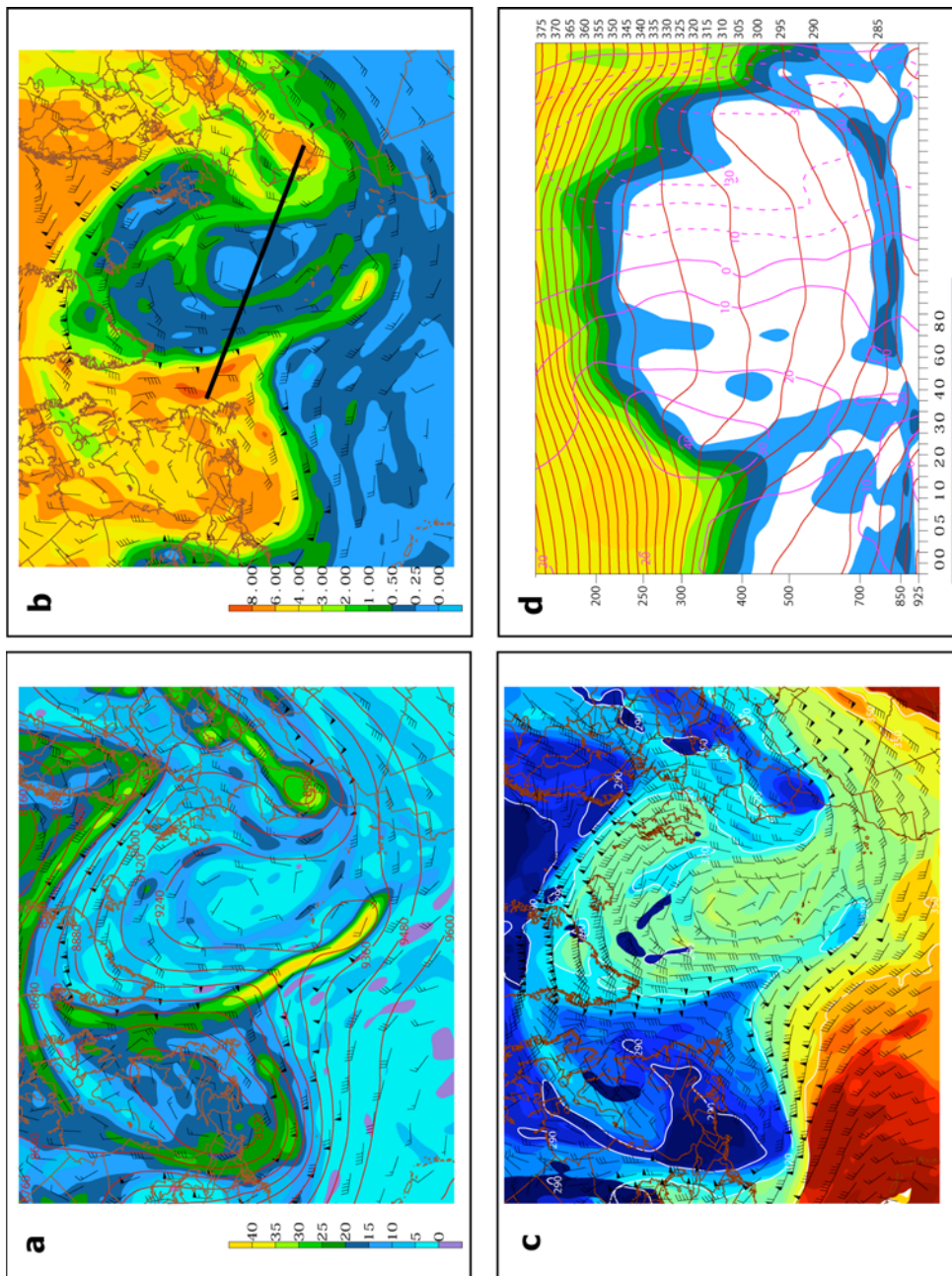


Figure 2.1. Example of a North Atlantic blocking event from 1200 UTC 26 January 2007. (a) 300-hPa absolute vorticity (shaded), geopotential height (contoured, interval 120 m) and wind (ms^{-1}); (b) Ertel PV (PVU, shaded) and wind (ms^{-1}) in the 315-325 K isentropic layer; (c) isertelic (1.5 PVU surface) analysis of potential temperature (filled, interval 5 K) and wind (ms^{-1}); (d) cross-section shown in panel (b) showing Ertel PV (shaded), normal winds (purple, interval 10 ms^{-1}) and potential temperature (red, interval 5 K).

Azores, with a dramatic jet split on the western flank of the ridge. At this time, the event was a classic omega-block, with vorticity maxima on either side of the base of the ridge.

The 315-325 K isentropic layer Ertel potential vorticity¹ (PV) for the same blocking event is shown in Fig. 2.1b. In this layer, throughout most of the blocking ridge, the PV was uniformly below 0.5 PVU, as also shown for specific blocking cases by Illari (1984) and Crum and Stevens (1988). The structure of the block on the dynamic tropopause (Fig. 2.1c) is shown on the 1.5 PVU isertelic analysis (Morgan and Nielsen-Gammon 1998). Potential temperature along the dynamic tropopause (hereafter TPT) acts as a dynamical tracer while also portraying intricate details over nearly all portions of the Northern Hemisphere, no matter the pressure surface on which the tropopause lies. A raised tropopause (high 1.5 PVU potential temperature) and broad anticyclonic circulation defines the blocking ridge, around which is a substantial TPT gradient. A trough, or depressed tropopause, was positioned over the Strait of Gibraltar, with a region of high TPT breaking anticyclonically to its north over the British Isles.

Figure 2.1d is a nearly east-west cross-section through the block, with its position shown in Fig. 2.1b. To the west of the block, the dynamic tropopause was at approximately 400 hPa, and rose to nearly 200 hPa within the blocking ridge. A strong southerly (northerly) jet, with a maximum of 40 m s⁻¹ was located on the western (eastern) side of the ridge in association with a strong horizontal PV gradient, along with a marked spreading of the

¹ The Ertel PV (q), used is defined as $q \equiv \frac{1}{\rho} \bar{\omega} \cdot \nabla \theta$, where ρ is the density, $\bar{\omega}$ is the absolute vorticity vector, and θ represents the potential temperature.

isentropes. At this stage in the block's life-cycle, the jet features extended to the lower troposphere, as the block was characterized by an equivalent barotropic structure.

Blocking has a major impact on regional temperatures and precipitation. Typically, relatively warm and dry weather exists beneath the blocking anticyclone, where large positive upper-tropospheric height anomalies are located. To the south, a cut-off upper-tropospheric low often occurs with blocking events (dipole blocks), which is associated with a prolonged period of cool and wet weather (Rex 1950; 1951; Petterssen 1956). The duration of blocking events can often last for several weeks, making the conditions associated with them especially problematic.

Important precursors to block development are an upper-tropospheric diffluent jet (Colucci 2001) and enhanced baroclinic wave activity upstream (Nakamura and Wallace 1990; 1993). Additionally, Shutts (1983; 1986) showed that the presence of a strong deformation field within a pre-existing jet causes synoptic-scale eddies to become zonally compressed and meridionally elongated. This process enhances the momentum flux into the block, and acts as a self-maintaining mechanism which enables the blocking anticyclone to sustain itself for a long duration.

Recent research has also shown a strong connection between explosive cyclogenesis events and downstream block development. Konrad and Colucci (1988) hypothesized that the critical condition for the onset of blocking may be the long duration, meridional transport of air parcels immediately following surface cyclogenesis upstream. Nakamura and Wallace (1993) suggested that the low PV within a blocking anticyclone originates in the tropics, and is simply advected poleward downstream of an intense surface cyclone. Lackmann et al. (1996) analyzed rapidly deepening cyclones over the western North Atlantic in order to study

the synoptic- and planetary-scale environment associated with explosive cyclogenesis. It was shown that the wavelength between the amplifying trough and downstream ridge associated with rapid cyclogenesis decreases significantly. This characteristic of explosive cyclogenesis events helps to enhance the meridional part of the flow, which increases the likelihood for a blocking event to occur through the poleward advection of low PV.

Isentropic analyses of blocking events have been examined in order to further investigate the roles of synoptic-scale processes in the onset and maintenance of a blocking anticyclone (Illari 1984; Lackmann et al. 1996; Colucci 2001; Schwierz et al. 2004; Dong and Colucci 2005). Illari (1984) demonstrated that low values of upper-tropospheric PV are advected poleward into a block at the jet split. This falls in accordance with research by Mahlman (1979) and Nakamura and Wallace (1993), which showed that rapid intensification of a blocking anticyclone occurs when an anticyclonic eddy advects low PV air into the western flank of the block from low to mid latitudes.

That there exists a relationship between (explosive) upstream cyclogenesis and blocking onset, and that explosive cyclogenesis is associated with considerable latent heating (Reed et al. 1988) suggests a link between significant *synoptic-scale* latent heating and block formation. The Lagrangian tendency of PV is given by:

$$\frac{Dq}{Dt} = \frac{1}{\rho} \bar{\omega} \cdot \nabla \dot{\theta} + \frac{1}{\rho} \bar{\omega} \cdot (\bar{\nabla} \times \mathbf{F})$$

where $\dot{\theta}$ represents the diabatic heating rate and \mathbf{F} represents a frictional force. In the Northern Hemisphere, for a mid-tropospheric heating maximum, the PV tendency equation diagnoses a Lagrangian decrease in PV in the upper troposphere, and an increase in PV in the lower troposphere. Thus, after large amounts of latent heating, a dramatic decrease in upper-

tropospheric PV results in a stronger anticyclonic circulation aloft. The destruction of low PV aloft in a Lagrangian sense may only occur diabatically, such as through radiational cooling. Thus, the presence of a latent heating-induced low upper-tropospheric PV anomaly can endure for several days. As a result, it is hypothesized that some of the low PV within a block originated through latent heat release. The primary focus of this work is the importance of the role of latent heat release associated with rapidly deepening cyclones or active frontal boundaries on the development and maintenance of a block.

Recent research has indeed shown that there may be a link between diabatic heating and block formation. Crum and Stevens (1988) analyzed a case of North Atlantic blocking and demonstrated that latent heating dramatically affected the path of air parcels as they moved into the anticyclonic region of the block. By simulating a block with and without condensational heating, they found that parcels affected by latent heating acquired a much more amplified anticyclonic circulation, and moved more poleward than parcels experiencing no latent heating. Due to the importance of latent heating as well as the advection of low PV from low latitudes east of a strong cyclone, it was concluded that developing cyclones may play an important role in the development of North Atlantic blocking. Additionally, Schwierz (2001) showed that the low PV (<1 PVU) within a blocking anticyclone is partially induced through latent heating. Through analysis of a North Atlantic blocking case from January 1987, it was shown that 80% ($>20\%$) of 72-hr trajectories ending within the blocking anticyclone are cross-isentropic with a change in potential temperature of more than 5 K (20 K), and that less than 20% of trajectories ending within the blocked region of PV < 0.5 originated in the tropics. Thus, it was proven that the January 1987 blocking case was almost entirely diabatically forced.

Through investigation into the origin of the low PV within two blocking events, this study will further analyze and offer a dynamical interpretation of the role of latent heating on the formation and maintenance of blocking events. In section 2.2, an adaptation of the recent PV- θ based blocking index created by Pelly and Hoskins (2003) will be used to identify recent cases of North Atlantic blocking. Two cases of North Atlantic blocking episodes will be analyzed in section 2.3. Section 2.4 describes simulations of each event with and without the effects of condensational heating, and in section 2.5, the use of an adjoint model will be employed in identifying areas particularly sensitive to the low PV within a specific blocking anticyclone.

2.2 Data and blocking case retrieval methodology

a. Data sets

The principal data sets used in this study are six-hourly global tropospheric analyses archived at the National Center for Atmospheric Research as datasets ds090 and ds083.2. Dataset ds090 is the $2.5^\circ \times 2.5^\circ$ NCEP/NCAR reanalysis (Kalnay et al. 1996) and dataset ds083.2 is the $1.0^\circ \times 1.0^\circ$ National Centers for Environmental Prediction (NCEP) final analysis. The former was used for analysis of the February 1983 blocking event, and the latter for use in retrieval of blocking cases from 2000-2007, and in analysis of the January 2007 event.

b. Blocking indices in recent research

An important initial step in blocking research is the creation of an index capable of identifying occurrences of blocking. These blocking indices have traditionally been based on

criteria similar to that of Rex (1950; 1951). Because blocking is associated with a persistent, anomalous anticyclonic circulation poleward of the climatological jet position (dipole blocking), many blocking indices are based on upper-tropospheric geopotential height differences between two latitude bands. Lejenäs and Økland (1983) identified blocking episodes by calculating the height difference between 40° N and 60° N every 10° latitude around the globe. In their index, a negative height difference between 40° N and 60° N was classified as blocked flow. Dole and Gordon (1983) identified blocking as persistent large-scale geopotential height anomalies in the upper troposphere, and used this method of identification in order to find preferred geographic regions of such anomalies. More recent studies of blocking have incorporated the more subjective criteria put forth by Rex (1950; 1951) coupled with the index proposed by Lejenäs and Økland (i.e., Wiedenmann et al. 2002) such that blocking distribution, frequency of occurrence, and intensity can be analyzed.

Because a blocking anticyclone is associated with a broad region of anomalously low PV, more recent blocking indices have used PV as the principal diagnostic variable for identifying blocking events. Schwierz et al. (2004) defined blocking episodes as the occurrences of negative upper-tropospheric (150 – 500-hPa) column-averaged PV anomalies lasting for longer than 5 days. Pelly and Hoskins (2003, hereafter referred to as PH) created an index based on the meridional reversal of potential temperature along the dynamic tropopause (hereafter, TPT). This index captures events with an anomalous latitudinal dipole of PV or TPT (anticyclonic PV poleward of cyclonic PV), and also has a greater ability to identify omega-blocks than a traditional height-based index.

c. Blocking event identification

In order to identify cases of blocking in the North Atlantic in this thesis, an adaptation of the index developed by PH was used. The index is based on the fact that blocking development is often associated with anticyclonic Rossby wave breaking events, wherein anomalously anticyclonic, upper-tropospheric PV is advected poleward, and anomalously cyclonic PV is advected equatorward by a large anticyclonic gyre. This circulation configuration results in a PV arrangement with anomalous anticyclonic PV (high TPT) found poleward of anomalous cyclonic PV (lower TPT). The blocking index of PH is based on the persistent nature of this arrangement of PV (TPT).

Figure 2.2 is a schematic depicting the application of the index used in this study. Because this paper focuses on blocking in the North Atlantic, the index was used only in the Northern Hemisphere. As in PH, the difference between the average TPT in the northern box and the average TPT in the southern box defines the index, though in this study, the tropopause is instead defined as the 1.5 PVU surface. If the average TPT in the box to the north is greater than the average TPT in the southern box, the center point (labeled X) is considered instantaneously blocked. The dimensions of the boxes are based on the typical structure of a block. Following PH, 30° was chosen for $\Delta\phi$, an approximation for the meridional scale of a block. As a result, both boxes used to calculate the blocking index have a meridional length of 15° latitude. The longitudinal scale used in calculating the blocking index ($\Delta\lambda$) was 17° . This enables the blocking index to capture large synoptic-scale patterns, and accommodates for small longitudinal spacing at high latitudes.

Using the $1^\circ \times 1^\circ$ NCEP final analysis gridded data, the blocking index schematic shown in Fig. 2.2 was applied from 17° N to 75° N (due to the longitudinal constraints of the

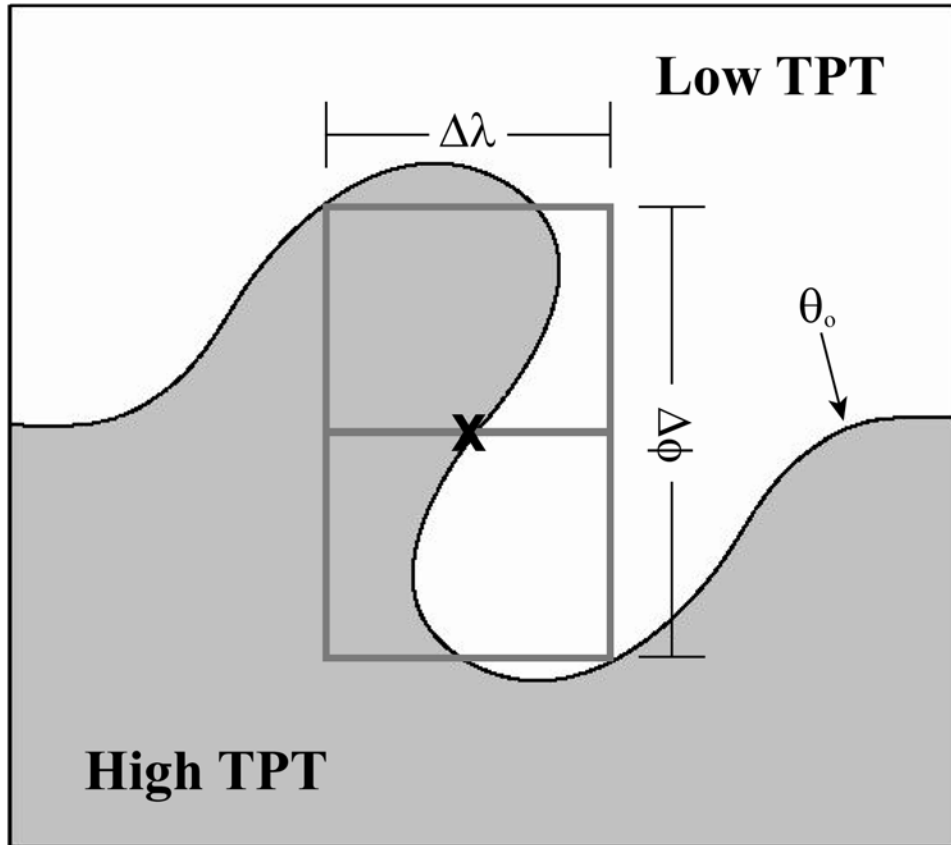


Figure 2.2. Blocking index schematic showing idealized blocked flow with high TPT shaded, where θ_0 is an isentrope on the 1.5 PVU surface. $\Delta\lambda$ and $\Delta\phi$ represent the latitudinal and longitudinal extent of the boxes used to define the index.

index itself) with center points placed at each grid point. Figure 2.3 shows the number of “events” (locations with a positive index for five days) for the period from November 2000 – March 2007 (NDJFM only). This figure simply depicts a count of the occurrence of five day events at each point. Thus, an event with a duration of longer than five days is counted as multiple events.

While the event count in Fig. 2.3 does bear some resemblance to recent studies of block climatology (Schwierz et al. 2004; Barriopedro et al. 2006), there are some important differences. A striking number of events were identified over eastern Russia and the northwest Pacific. In addition, a local maximum was centered over northern Labrador and northeast Quebec. Neither of these regions is typically favorable for the occurrence of blocking events (Lejenäs and Økland 1983; Barriopedro et al. 2006). Upon further investigation, the events identified in the aforementioned regions bear little resemblance to blocking events, but rather are often associated with a cut off region of anomalously high TPT to their north. Because the high TPT is displaced from the mid-latitude storm track region, they are not associated with blocks, even though their structure is identified as a block through this TPT-based index. Berrisford et al. (2007) described these as high-latitude cyclonic wave-breaking events that do not act to block the mean westerly flow. Woollings et al. (2008) applied the PH index throughout the Northern Hemisphere, and displayed very similar results to Fig. 2.3. Their analysis also showed that the high-latitude events over Siberia and eastern Canada are associated with cyclonic wave-breaking episodes not resembling a classic block.

While the index captures many events that bear little resemblance to classic blocking, another regional maximum in the 5-day event count is centered over northern Europe and the

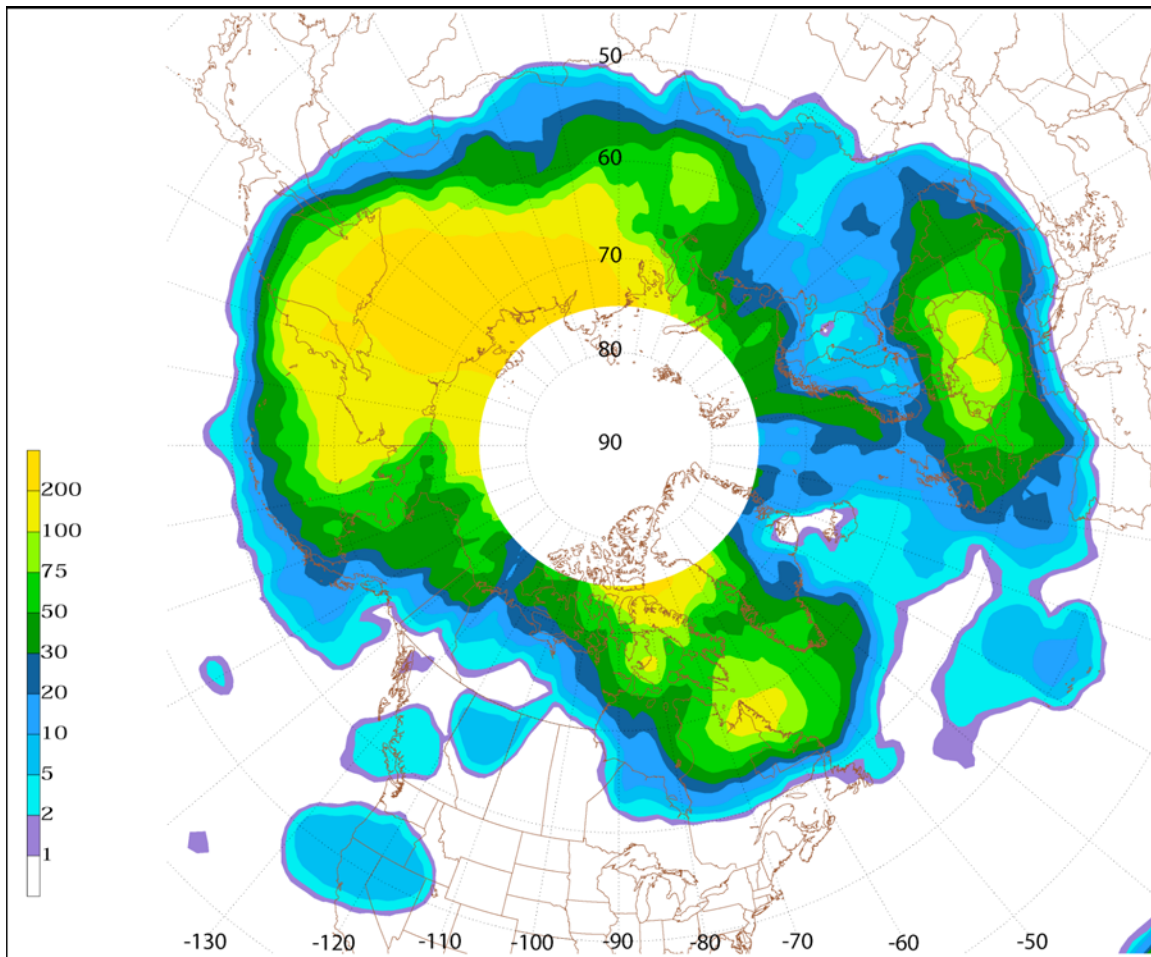


Figure 2.3. Count of all 5-day blocking periods from November 2000 – March 2007 (NDJFM only) using the blocking index described in section 2.

northeast Atlantic, a climatologically favorable location for block development (Schwierz et al. 2004; Barriopedro et al. 2006). The majority of these events are blocking events, usually with a persistent cut off low to the south of a broad, anomalous anticyclone. Even though the index used in this study identifies events not typically classified as blocks, the event shown in Fig. 2.1 was identified as a blocking event using the index described in this section. Specifically, Fig. 2.1c clearly shows the meridional reversal of TPT over western Europe. It is this region that the index identified as being blocked, due the persistent, stationary nature of the TPT dipole.

d. North Atlantic blocking events

Because this study focuses specifically on blocking events in the North Atlantic, a subset of the data shown in Fig. 2.3 was used in creating a list of blocking cases to analyze. In order to identify blocking cases across the North Atlantic, as well as those events occurring within the local maximum over northern Europe, the area chosen to identify blocking events lies from 60° W to 11° E, and from 42° N to 57° N (as shown in Fig. 2.3). The latitudinal bounds follow the analysis of a central blocking latitude in the North Atlantic by PH. In order to account for the movement of the block, an adjacent blocked point counts as the same event. Because the development of the blocking event is crucial in this study, any event that originated at the western boundary (60° W) was discounted, as its development may have partially occurred west of 60° W. Additionally, if there was an overlap between two events (i.e., one event began in the western part of the domain as another was ongoing in the east), the second event was neglected for similar reasons. The author acknowledges that some prominent blocking events from the time period analyzed

will be missing from the event list due to these constraints. However, this method was the simplest way to ensure that each event develops within the region analyzed, and that each case is temporally isolated. Table 1 shows the list of blocking events from November 2000-March 2007 (NDJFM only) that were identified using this methodology. Cases marked with an asterisk are those that do not resemble a blocking pattern, but are associated with a cut-off anticyclonic circulation or high-latitude wave-breaking event, as described in section 2.2b.

2.3 Case Studies

In order to investigate the role of latent heating in the formation and maintenance of a block, two cases will be analyzed. First, an event from February 1983 associated with an extraordinarily anomalous blocking ridge will be discussed. Next, one of the more impressive and persistent events from the list of blocking cases found using the index described in section 2.2 will be analyzed.

As described in section 2.1, Lagrangian changes of PV on an isentropic surface are associated with friction or diabatic processes. The same is true for TPT, as it is also an adiabatically conserved variable. Thus, sequences of dynamic tropopause maps are inherently useful for depicting regions of PV or potential temperature non-conservation. As will be shown for both cases, the importance of latent heating in building the blocking ridge is readily seen using such an analysis. The dynamic tropopause maps in this paper are created using the contour superposition method described by Morgan and Nielsen-Gammon (1998).

Table 2.1

Case	Start date	End date	Duration	Longitude
1	10 Jan 2001	21 Jan 2001	12	5W – 11E
2	18 Feb 2001	23 Feb 2001	6	10W – 6W
3	24 Feb 2001	1 Mar 2001	6	44W – 37W
4	13 Nov 2001	20 Nov 2001	8	11W – 4W
5	6 Dec 2001	19 Dec 2001	14	10W – 11E
*6	3 Jan 2002	9 Jan 2002	7	9E
*7	10 Jan 2002	15 Jan 2002	6	9E – 11E
*8	23 Jan 2002	29 Jan 2002	7	49W – 37W
9	2 Mar 2002	8 Mar 2002	7	10W – 2W
*10	15 Mar 2002	21 Mar 2002	7	42W – 27W
11	2 Dec 2002	13 Dec 2002	12	8W – 11E
12	6 Jan 2003	15 Jan 2003	10	3W – 8E
13	7 Feb 2003	21 Feb 2003	15	2W – 11E
*14	6 Mar 2003	11 Mar 2003	6	57W
15	13 Mar 2003	20 Mar 2003	8	4E – 11E
16	5 Nov 2003	10 Nov 2003	6	10E – 11E
17	1 Dec 2003	11 Dec 2003	11	19W – 6E
18	18 Feb 2004	24 Feb 2004	7	11W – 9W
19	7 Mar 2004	12 Mar 2004	6	8E
20	24 Mar 2004	29 Mar 2004	6	10W – 6W
*21	6 Nov 2004	11 Nov 2004	6	8E – 10E
22	2 Dec 2004	11 Dec 2004	10	7W – 4E
23	24 Jan 2005	2 Feb 2005	10	0 – 11E
24	13 Feb 2005	20 Feb 2005	8	26W – 22W
25	9 Dec 2005	17 Dec 2005	9	4W – 4E
26	1 Jan 2006	10 Jan 2006	10	3E – 11E
27	24 Jan 2006	2 Feb 2006	10	12W – 7E
28	20 Feb 2006	27 Feb 2006	8	13W – 3E
29	15 Mar 2006	20 Mar 2006	6	23W – 15W
30	18 Dec 2006	27 Dec 2006	10	6W – 11E
31	22 Jan 2007	2 Feb 2007	12	15W – 4W
*32	21 Feb 2007	27 Feb 2007	7	56W – 53W
33	19 Mar 2007	-	-	1W – 11E

a. February 1983 case

One of the most widely studied cases of North Atlantic blocking is the event from February 1983 (Shutts 1986; Mak 1991; Morgan et al. 1991). During a three week period in February 1983, several major cyclogenesis events occurred over the eastern United States, Canada, and the northwest Atlantic, including a major snowstorm on 11-12 February which affected the major east coastal cities of the United States. The first of these events occurred on 2 February 1983, as an intensifying cyclone and strong cold front moved across the eastern United States, producing flooding rains over the southeast United States. Morgan et al. (1991) first suggested the importance of latent heating associated with this cold front in the formation of the block.

Figure 2.4a shows 300-hPa geopotential height and winds, and sea level pressure for the pre-blocking environment at 0600 UTC 2 February 1983 using NCEP reanalysis data. A negatively tilted 300-hPa trough with winds greater than 35 m s^{-1} at its base was located over the south central United States. A developing cyclone with a minimum sea level pressure of 996 hPa was centered over southeast Missouri, at the inflection point between the aforementioned upper trough and downstream ridge. In addition, a 300-hPa trough was centered over Newfoundland.

24 hours later, the surface cyclone had deepened to 990 hPa, and was centered near Grand Rapids, Michigan (Fig. 2.4b). The cyclone was vertically stacked and occluded, with a cold front positioned across the southeast United States. At 300 hPa, the ridge had amplified dramatically, and the jet streak had increased in strength to 70 m s^{-1} . Additionally, a 300-hPa geopotential height minimum was located due west of the Azores. By 0000 UTC 4 February 1983, the 300-hPa ridge had begun to break anticyclonically to the north of the

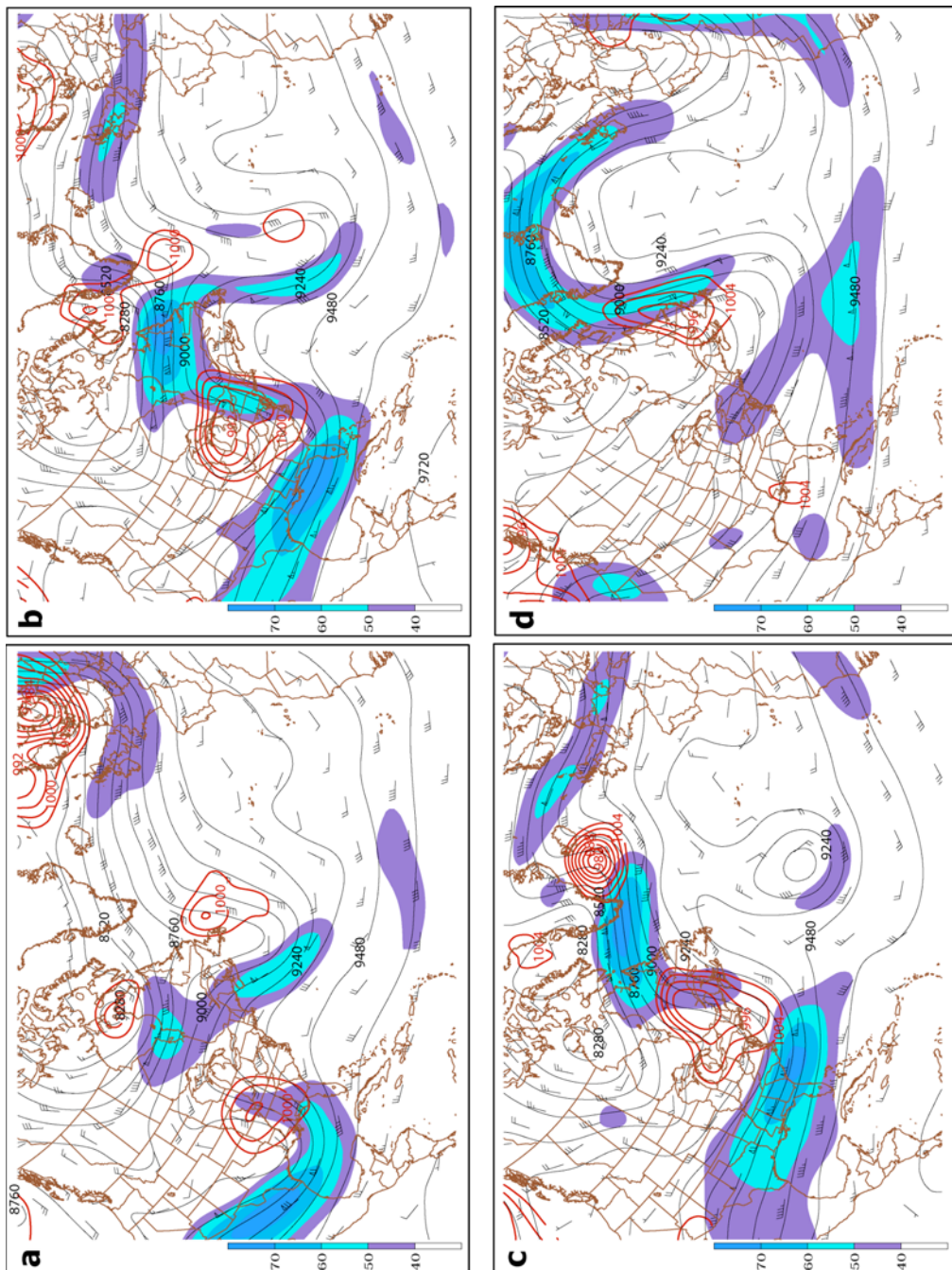


Figure 2.4. 300-hPa geopotential height (black contours, interval 120 m), isotachs (colored fill, ms^{-1}), and sea level pressure 1004 hPa and below (red contours, every 4 hPa) for (a) 0600 UTC 2 Feb; (b) 0600 UTC 3 Feb; (c) 0000 UTC 4 Feb; (d) 1200 UTC 10 Feb.

aforementioned upper trough, now positioned southwest of the Azores (Fig. 2.4c). Near Bermuda, significant 300-hPa geostrophic diffluence was evident downstream of a 70 m s^{-1} jet, a characteristic of a blocking pattern.

Throughout the evolution of this event, several cyclogenesis events took place upstream from the blocking ridge. These events aided in amplifying the blocking ridge dramatically as it transitioned into an omega-block structure. By 1200 UTC 10 February, the blocking ridge extended to nearly 80° N (Fig. 2.4d), and 300-hPa height anomalies exceeded 600 m southeast of Greenland (not shown). The blocking pattern gradually moved east and lasted until 20 February.

That the building of the blocking ridge occurred in conjunction with significant upstream latent heating can be shown using a sequence of dynamic tropopause maps. Rather than using the coarse $2.5^\circ \times 2.5^\circ$ gridded reanalysis data to show the evolution of the block on the dynamic tropopause, a 60-h simulation of the event using the fifth-generation Pennsylvania State University-National Center for Atmospheric Research (PSU-NCAR) Mesoscale Model, version 3 (MM5v3; Grell et al. 1995) on a 45 km, 216×160 horizontal grid, with 23 sigma layers is used. This simulation uses the Kain-Fritsch 2 cumulus parameterization, and was initialized with NCEP reanalysis data at 0000 UTC 2 February 1983, just prior to the development of heavy precipitation along the cold front over the southeast United States. A comparison of the simulation at forecast hour 48 (Fig. 2.5) with the reanalysis data valid at the same time (Fig. 2.4c) shows a very similar upper-tropospheric structure. Additionally, a comparison of the average precipitation rates over 24 and 48 hour periods (Figs. 2.6b and 2.6d respectively) with the NCEP/NCAR reanalysis precipitation rate for the same two periods (Figs. 2.6a and 2.6c) shows that the model captures the distribution

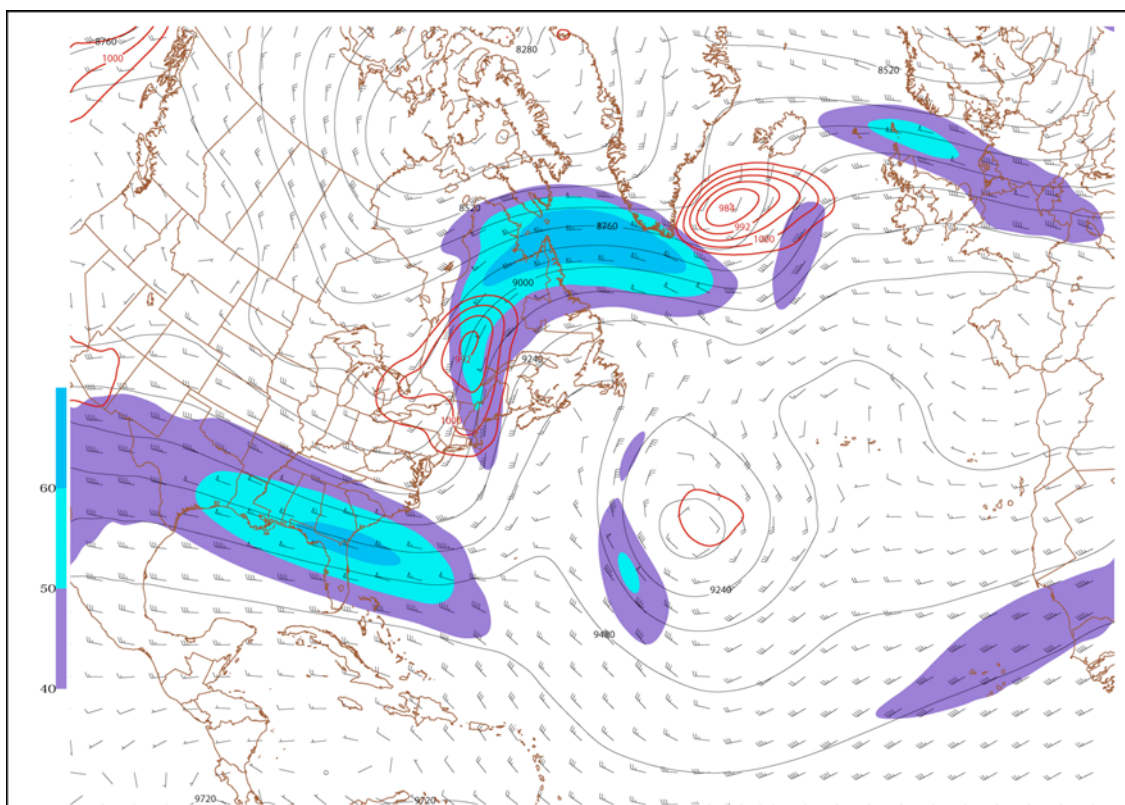


Figure 2.5. As in Fig. 4, but for the MM5 simulation at forecast hour 48 (0000 UTC 4 February 1983).

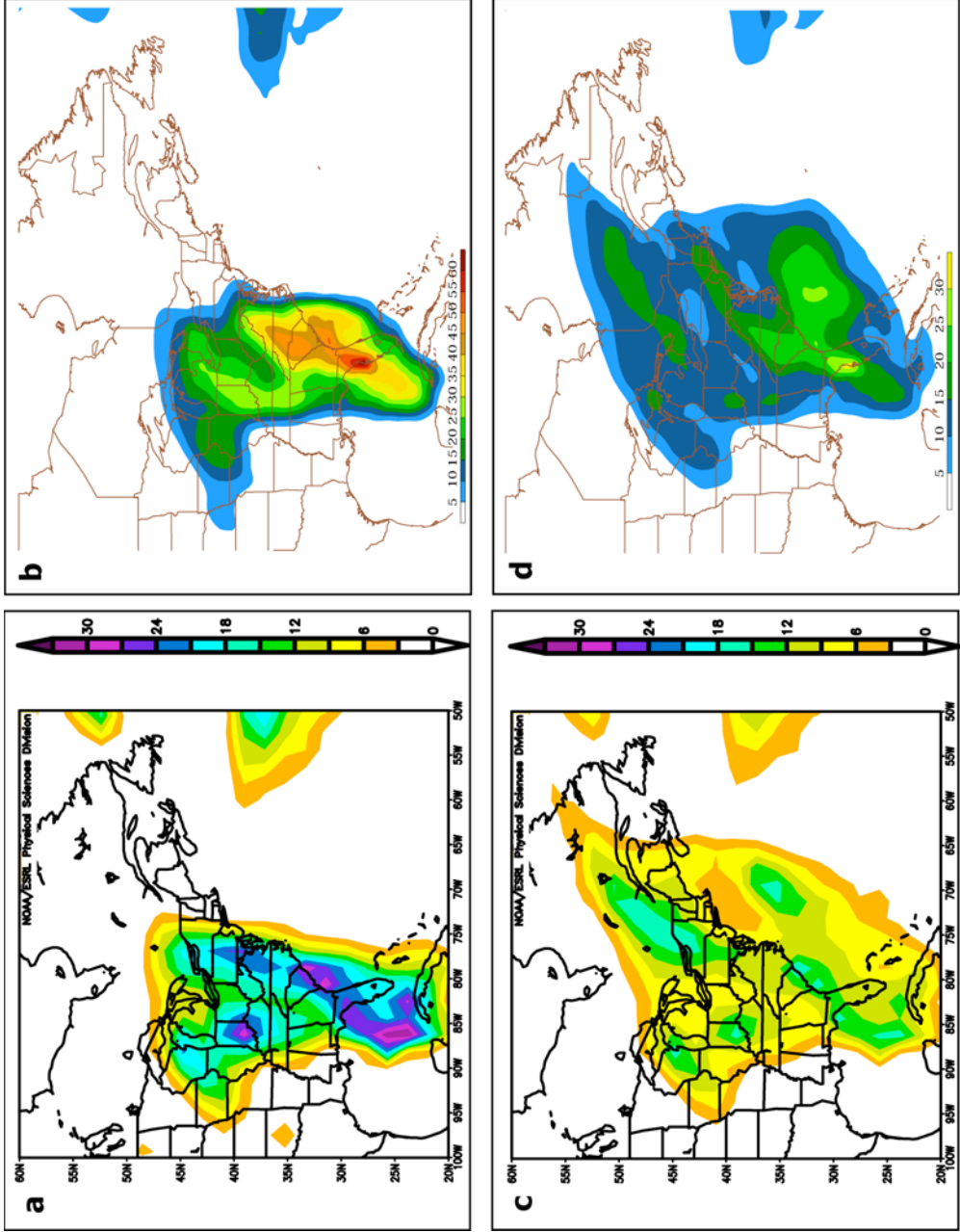


Figure 2.6. (a) 24-hour precipitation rate (mm day⁻¹) from 0000 UTC 2 Feb – 0000 UTC 3 Feb from NCEP reanalysis data; (b) As in Fig. 6a, but for the MIM5 simulation; (c) 48-hour average precipitation rate (mm day⁻¹) from 0000 UTC 2 Feb – 0000 UTC 4 Feb from NCEP reanalysis data; (d) As in Fig. 6c, but for the MIM5 simulation.

and intensity of the precipitation well during the initial 24 hours, but with slightly less accuracy during the following 24 hours.

The evolution of the block in the simulation is shown using dynamical tropopause maps (Fig. 2.7) and sea level pressure, 950-hPa temperature, and 6-hr accumulated precipitation (Fig. 2.8). At 0600 UTC 2 February, a pool of high TPT (low upper-tropospheric PV) associated with the amplifying ridge downstream from the intensifying cyclone was located over the eastern United States (Fig. 2.7a). As the surface cyclone intensified, heavy precipitation formed both near the cyclone center, and along the cold front (Figs. 2.8a and b). By 1800 UTC 2 February (Fig. 2.7b), a dramatic increase in TPT had occurred along the squall line and to the east of the surface cyclone on the western flank of the ridge. Furthermore, in the lower troposphere, an arc of low values of TPT appeared from northern Missouri to southwestern Quebec. That this change in TPT can not be explained through advection alone, and due to the appearance of high values of PV (low TPT) in the lower troposphere and low values of PV (high TPT) in the upper troposphere, suggests that diabatic processes have occurred. Indeed, the locations for the accumulated precipitation in the 6 hours ending at 1800 UTC 2 February are consistent with the locations of the TPT changes along the dynamic tropopause and in the lower tropospheric PV (low TPT) from Missouri to Quebec.

By 0600 UTC 3 February, the ridge had amplified dramatically, with TPT > 315 K as far north as northern Quebec (Fig. 2.7c). Additionally, the aforementioned region of high lower-tropospheric PV located north and west of the surface cyclone had grown in size. During the 6 hour period ending at 0600 UTC, the precipitation along the squall line and northwest of the cyclone center intensified (Fig. 2.8c). Again, the precipitation distribution

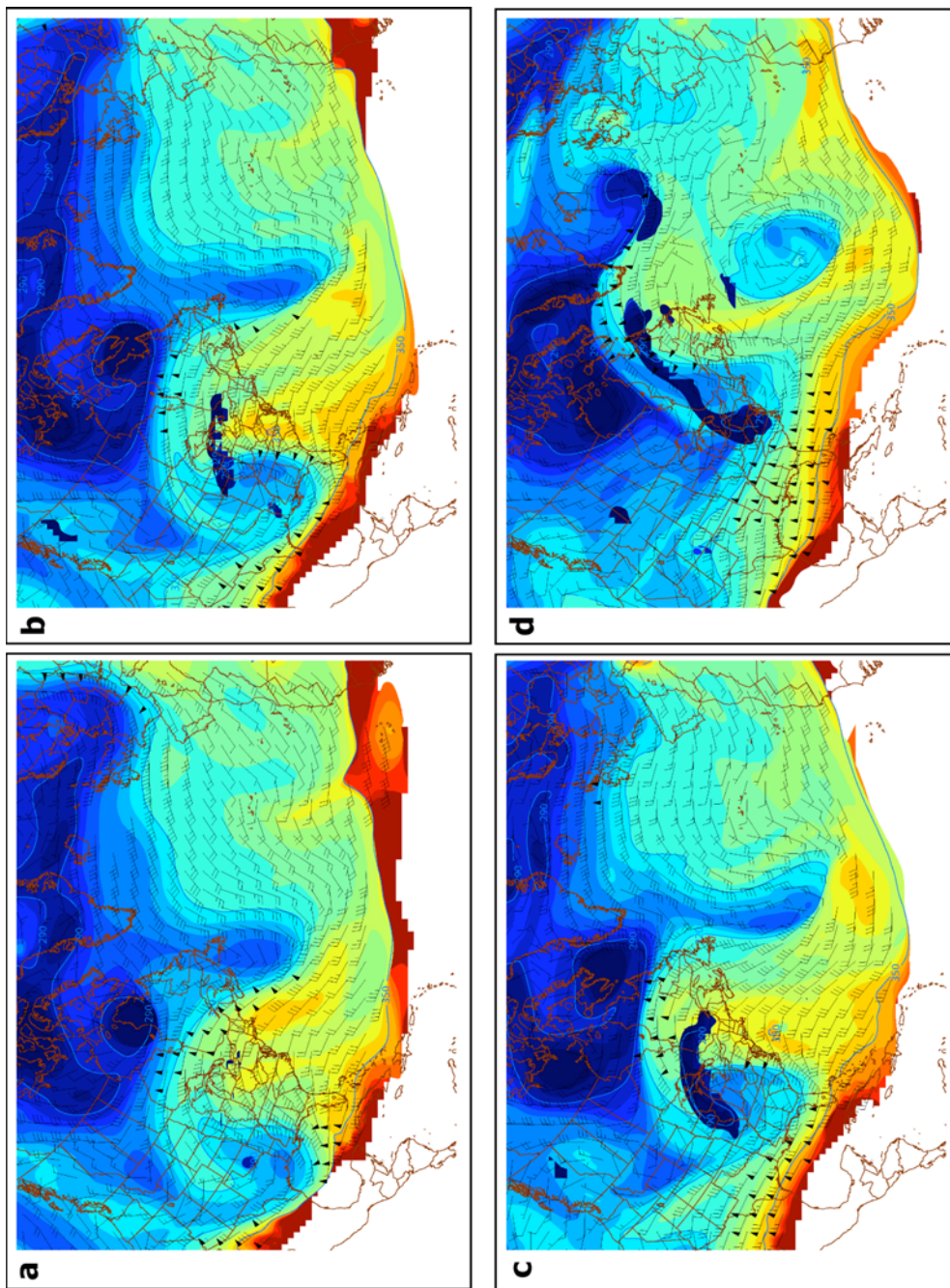


Figure 2.7. MM5 simulation of potential temperature on the dynamic tropopause (color filled, interval 5 K) and wind (ms^{-1}) for (a) 0600 UTC 2 Feb; (b) 1800 UTC 2 Feb; (c) 0600 UTC 3 Feb; (d) 1200 UTC 4 Feb.

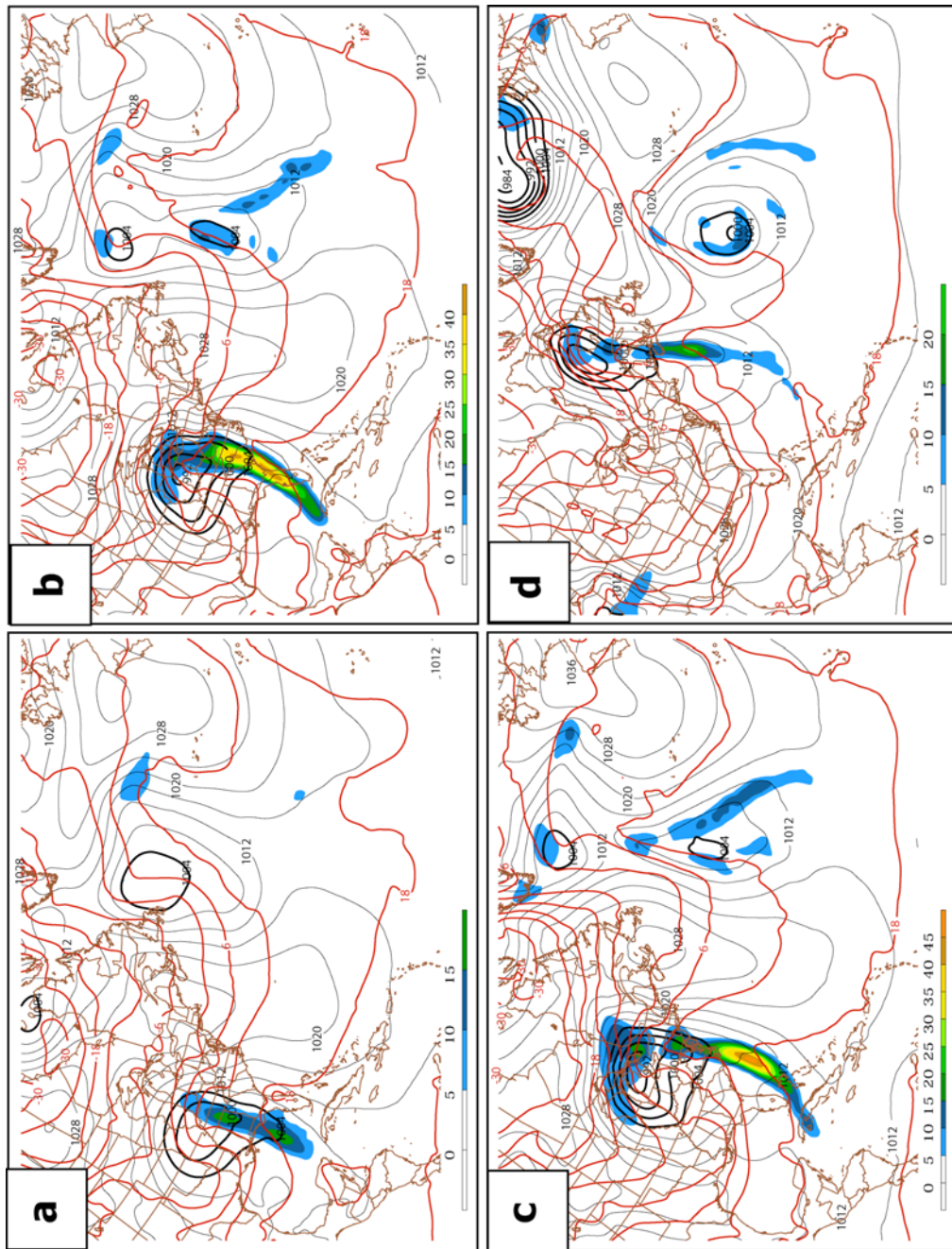


Figure 2.8. Model-derived 6-hour precipitation totals (color filled, interval 5 mm), sea level pressure (black contours, interval 4 hPa) and 950-hPa temperature (red contours, interval 6 °C) for (a) F6, (b) F18, (c) F30, and (d) F60.

and TPT changes are consistent with PV non-conservation. Finally, at 60 hours into the simulation (1200 UTC 4 February) the ridge had broken anticyclonically, north of the downstream trough (Fig. 2.7d). The precipitation associated with the squall line and cold front weakened during this period, and became meridionally elongated as the front encountered the intensifying downstream ridge (Fig. 2.8d). Near Bermuda, just west of the cut-off trough, the flow along the tropopause changed dramatically from being predominantly zonal to largely meridional. The circulation pattern on the tropopause clearly resembled a dipole blocking pattern. This pattern would ultimately transition to an omega-block structure and persist over the next two weeks, likely aided by additional cyclogenesis events.

b. January 2007 case

From the list of blocking events in Table 2.1, Case 31 was selected to be analyzed due to its relatively long duration and because it was a recent occurrence. As was the case preceding and during the February 1983 blocking event, several cyclogenesis events occurred upstream from the blocking ridge throughout the block's lifecycle. The first in the series of cyclones developed over the northeast United States and the maritime provinces of Canada, where torrential rains and heavy snows were reported. At Halifax, Nova Scotia, 48.8 mm of precipitation (mostly rain) fell on 19 January, and at Bathurst, New Brunswick, 39.0 cm of snow fell.

Figure 2.9a shows the 300-hPa height and winds, and sea level pressure at 1200 UTC 19 January 2007, and Fig. 2.9b shows the potential temperature along the dynamic tropopause at the same time. This time is 72 hours before block onset (1200 UTC 22

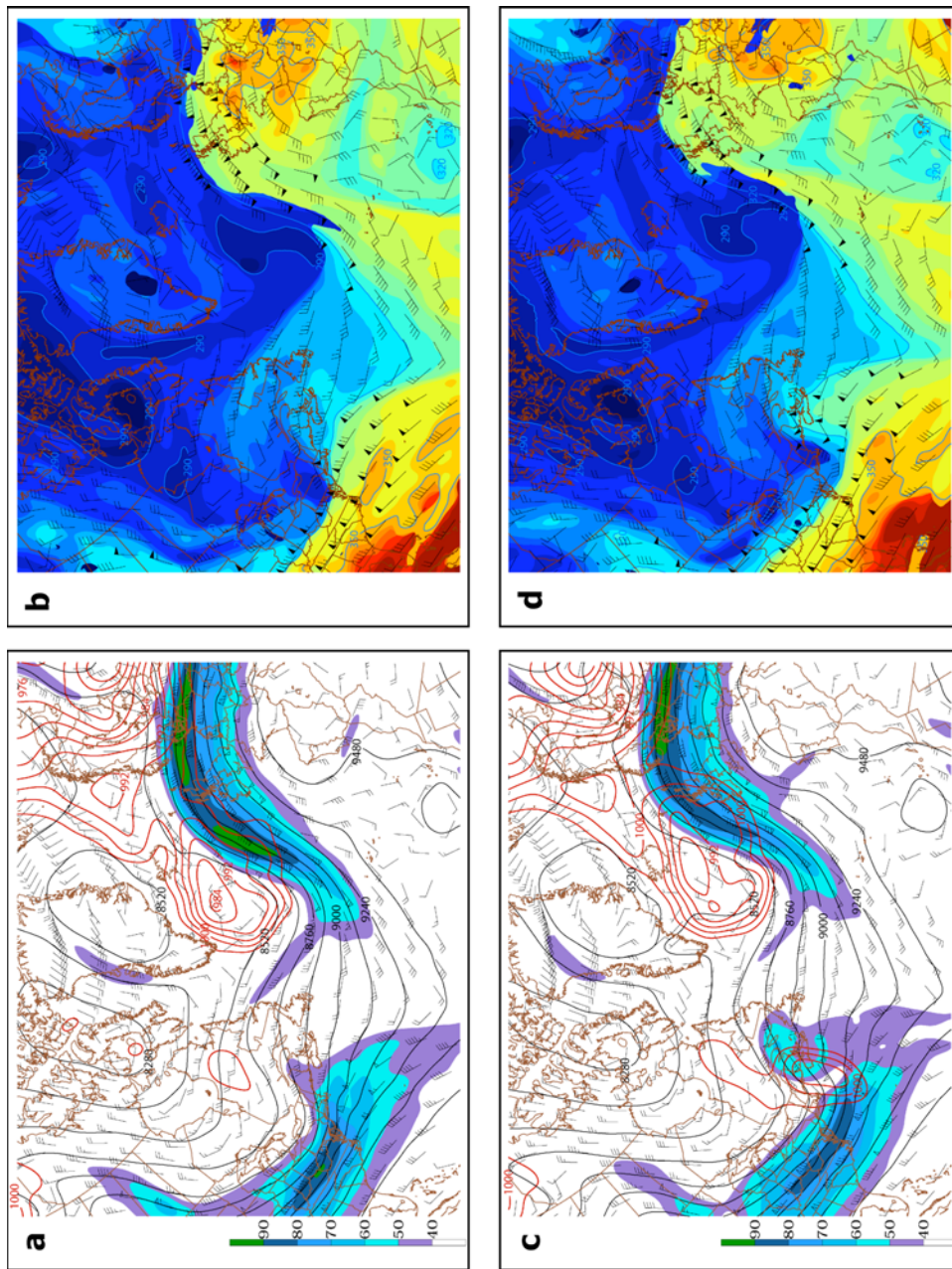


Figure 2.9. 300-hPa geopotential height (black contours, interval 120 m), isotachs (colored fill, ms^{-1}), and sea level pressure 1004hPa and below (red contours, every 4 hPa) for (a) 1200 UTC 19 Jan, and (c) 1800 UTC 19 Jan, and potential temperature on the dynamic tropopause (color filled, interval 5 K) and wind (ms^{-1}) for (b) 1200 UTC 19 Jan, and (d) 1800 UTC 19 Jan

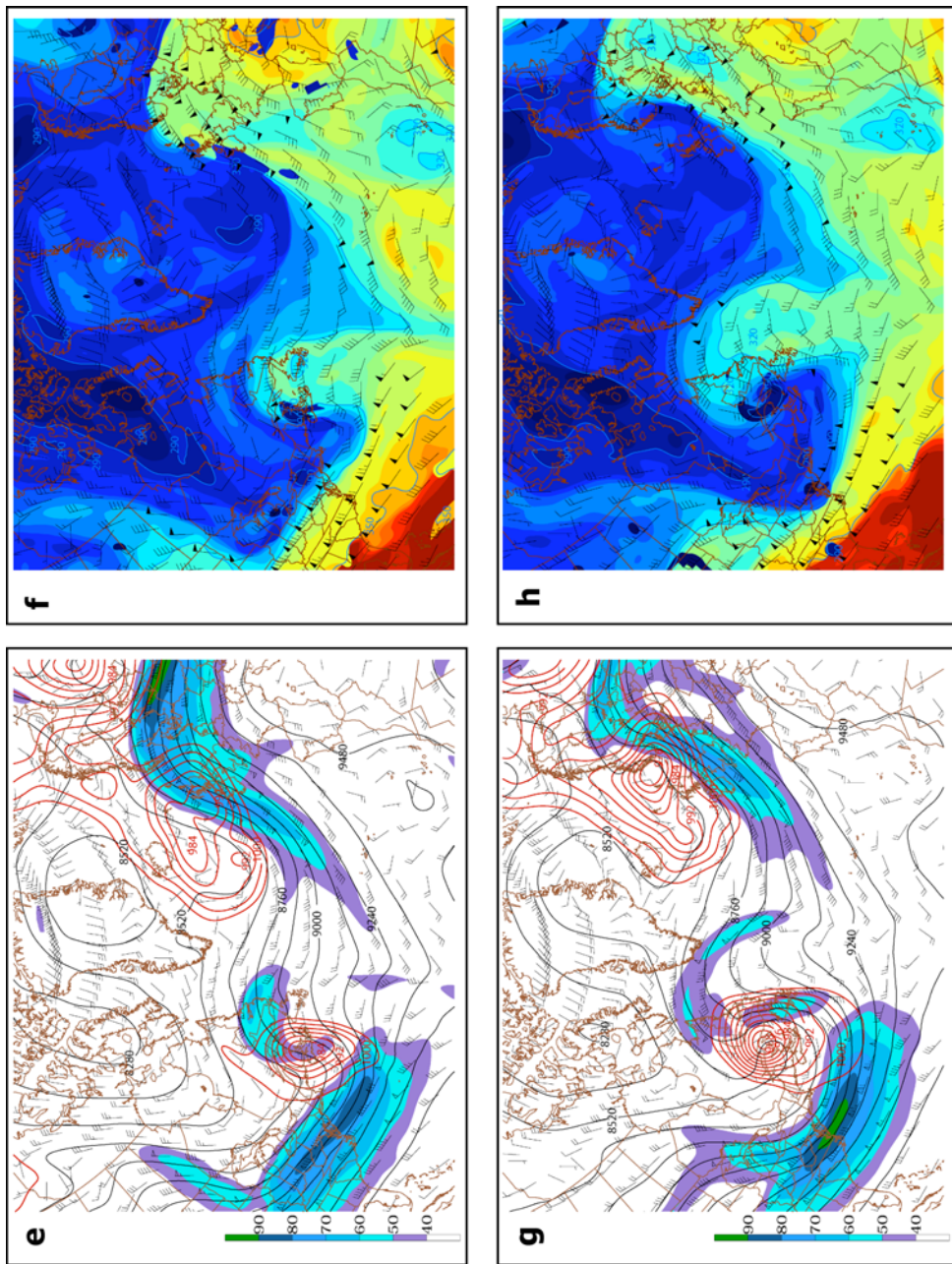


Figure 2.9 continued. As in Fig. 9a-d, but for (e and f) 0000 UTC 20 January, and (g and h) 1200 UTC 20 January

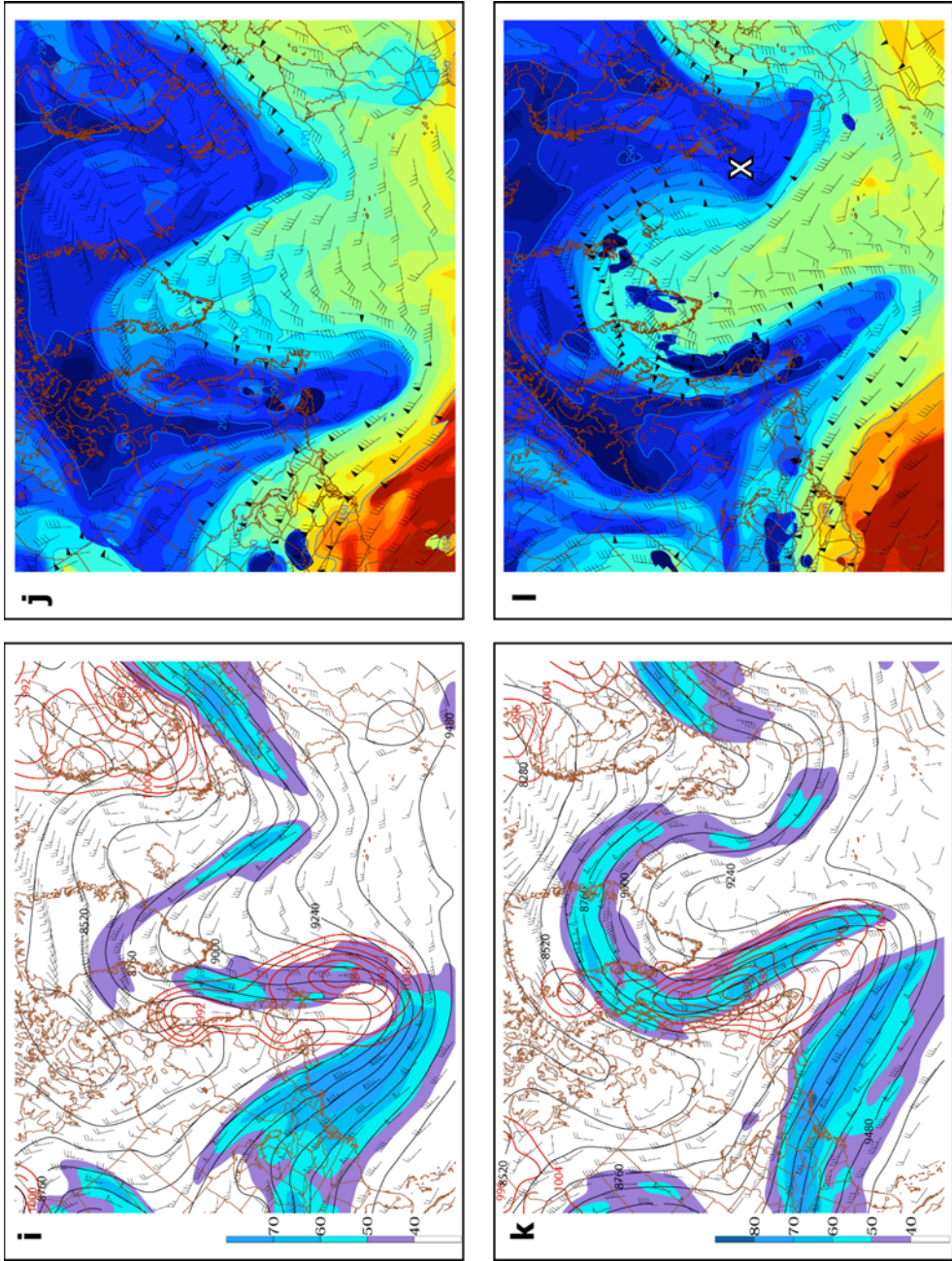


Figure 2.9 continued. As in Fig. 9a-d, but for (i and j) 1200 UTC 21 January, and (k and l) 1200 UTC 22 January. The X in Fig. 9l represents the first point (and time) at which the blocking index identified this case as a block.

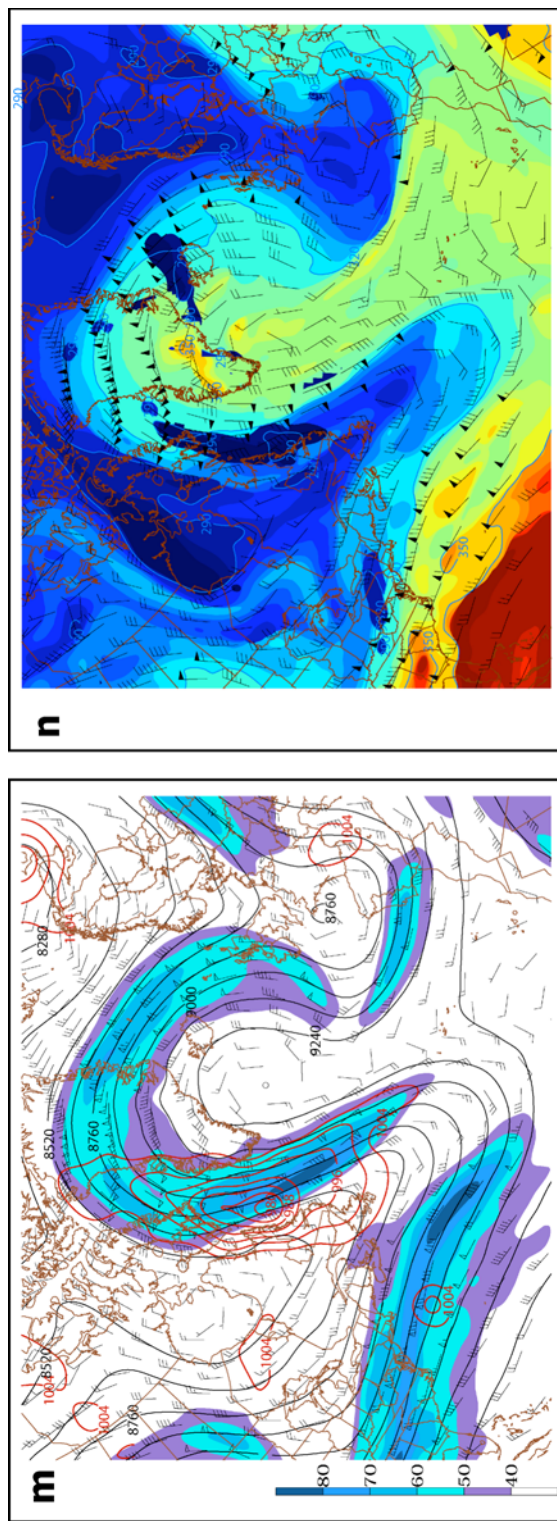


Figure 2.9 continued. As in Fig. 9a-d, but for (m and n) 0000 UTC 23 January

January), and thus depicts the synoptic pattern preconditioned for the development of the block. At this time, an 80 m s^{-1} , 300-hPa jet streak was positioned from southern Illinois to Delaware at the base of an upper trough. 300-hPa geostrophic diffluence was apparent downstream of this jet streak, a condition noted as being favorable for the development of a block (Colucci 2001). A surface cyclone was developing just downstream of the upper PV maximum (TPT minimum), with a minimum pressure of 1005 hPa. A strong TPT gradient collocated with the 300-hPa jet streak can be clearly seen in Fig. 2.9b. To the north of this tropopause fold was a region of particularly low TPT ($<300 \text{ K}$) centered over the central New York and Pennsylvania.

At 1800 UTC 19 January, the surface cyclone, centered just south of the Bay of Fundy, deepened to 993 hPa, having dropped an impressive 12 hPa in only 6 hours (Fig. 2.9c). Associated with this rapid pressure drop were large amounts of heavy precipitation over portions of southeast Canada and New England. Another distinct difference between the synoptic pattern at 1800 UTC and 1200 UTC was the sudden genesis of a $>50 \text{ m s}^{-1}$ jet streak over New Brunswick and the Gulf of St. Lawrence. The cause of this change is clearly seen on the dynamic tropopause (Fig. 2.9d). As in the February 1983 blocking case, examination of the Lagrangian changes of TPT gives credence to the fact that latent heating played an important role in the development of the January 2007 blocking event. At 1800 UTC, the TPT minimum (upper PV maximum) was located over Massachusetts. Downstream of this feature was strong curvature and an abrupt change from zonal to meridional flow. While this ridge could be seen on the tropopause at 1200 UTC (Fig. 2.9b), the curvature between the trough and ridge axes was far less apparent, and the TPT within the downstream ridge was much lower. As in the February 1983 case, these changes on the

tropopause within a six-hour period certainly cannot be explained by advection alone. Due to the intense precipitation falling at this time it is likely that latent heating resulted in a redistribution of tropospheric PV, lowering the PV aloft, and causing rapid genesis of the upper-tropospheric ridge. The rapid increase in TPT within the ridge helped to enhance the TPT gradient, resulting in an increase in the upper-tropospheric winds downstream of the cyclone's development, also aiding in the advection of low PV northward from lower latitudes.

At 0000 UTC 20 January, the surface cyclone's sea level pressure had dropped to 981 hPa (Fig. 2.9e), having deepened 24 hPa in only 12 hours. Its center was located over central Nova Scotia, remaining in a favorable position for continued intensification at the inflection point between the trough and ridge axes. Along the dynamic tropopause (Fig. 2.9f), the ridge had amplified even further, so that the northern periphery of the 315 K TPT extended as far north as southern Labrador. In addition, a region of $PV > 1.5$ existed at <290 K over New Brunswick at 0000 UTC, likely having been redistributed from the upper to lower troposphere through latent heating near the developing cyclone's center. That this lower tropospheric PV appeared on the western flank of the developing upper-tropospheric ridge strengthens the argument that the ridge was amplified through latent heating.

By 1200 UTC 20 January, the surface cyclone had deepened to 967 hPa (Fig. 2.9g). In a 24-hour period, the cyclone deepened 38 hPa in a 24-hour period, far surpassing the criterion for a "bomb," or explosive cyclogenesis event (Sanders and Gyakum 1980). Downstream of the surface cyclone, the 300-hPa ridge had begun to tilt negatively. On the tropopause, the ridge extended over 20° latitude, reaching the southern tip of Greenland (Fig. 2.9h). At the base of the ridge, there was a rapid transition from zonal to meridional flow,

and the block's split jet can be clearly seen. For future reference, it is important to note the existence of a secondary wave within the longwave trough. This was manifest as a region of positive curvature on the tropopause, located over northern Virginia.

By 1200 UTC 21 January, development of a secondary surface cyclone with sea level pressure of 983 hPa had occurred in direct association of the aforementioned secondary wave (Fig. 2.9i). Thus, while the first cyclone had filled to 992 hPa, the secondary shortwave and cyclone development continued to aid in advection of lower PV from the tropics, as well as additional tropospheric PV redistribution. At the tropopause, the northern portion of the ridge (a region of TPT > 310 K) was located as far north as central Greenland (Fig. 2.9j). Strong southerly winds continued to advect high TPT into the ridge.

According to the blocking index discussed in section 2.2, block onset occurred at 1200 UTC 22 January, which is shown in Figs. 2.9k and 2.9l. The blocking index identified this time as block onset due to the sudden anticyclonic breaking of the ridge, and thus the beginning of the persistent TPT dipole (high TPT poleward of low TPT) on the eastern side of the block. The X on Fig. 2.9l marks the point where the index discussed in section 2.2 first identified the event as a block. Though this point is somewhat far removed from the ridge, the anticyclone continued to break, further enhancing the meridional "reversal" of TPT. Additionally, the slight easterly component of the jet on the eastern flank of the block can be seen in Fig. 2.9k. 12 hours later, the ridge had become a very high-amplitude omega-block, as seen at 300 hPa and the dynamic tropopause (Figs. 2.9m and 2.9n, respectively). In the middle of the blocking ridge were isolated regions of very high TPT (greater than 350 K over parts of southern Greenland). Because these areas of low PV were far displaced from the tropics, it is very likely that they had been created through diabatic processes, and then

advected into the heart of the blocking ridge. At this time, it is now more clear that the low TPT air (low tropopause) had been rapidly advected clockwise around the blocking anticyclone producing a reversal in the meridional potential temperature gradient along the dynamic tropopause. Though the blocking ridge moved slightly east over the following ten days, the long-wave pattern remained persistent until the gradual demise of the blocking ridge and the transition to a more zonal flow over the north Atlantic.

2.4 Moist vs. dry simulations

In order to further investigate the role of latent heating in the formation of the two blocking events studied, model simulations with and without latent heating were compared. The non-hydrostatic, sigma-coordinate PSU/NCAR mesoscale model (MM5) was used in this study. For the February 1983 blocking case, 45 km grid spacing was chosen, while 40 km grid spacing was chosen for simulations of the January 2007 case. The vertical resolution for each simulation is 20 evenly-spaced sigma levels with a model top of 100 hPa. The 1983 simulation was initialized using reanalysis data while the 2007 simulation was initialized with the NCEP global tropospheric final analysis data. The models were initialized just prior to a time when diabatic heating presumably began to amplify the blocking ridge. Each moist simulation utilized the Kain-Fritsch 2 cumulus parameterization with a mixed phase moisture scheme. “Dry” simulations contained non-convective precipitation, but removed large scale saturation and rainfall evaporation (any process associated with latent heating).

Figures 2.10a and 2.10b show the dynamic tropopause at 60 hours into the moist and dry simulations of the February 1983 event, respectively. These simulations were initialized at 0000 UTC 2 February, approximately 18 hours prior to the strongest convective

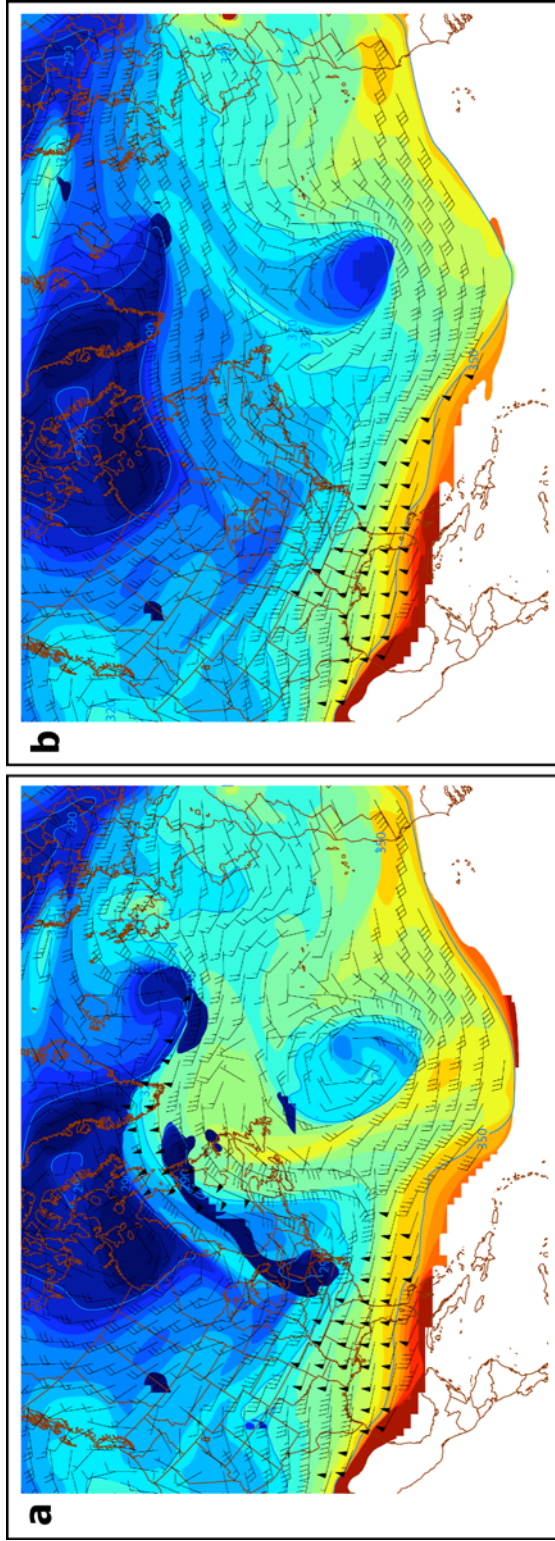


Figure 2.10. (a) Forecast hour 60 (1200 UTC 4 Feb) of the dynamic tropopause (as described in Fig. 9) for the “moist” simulation. (b) As in (a), but for the “fake dry” simulation.

precipitation along the squall line in the eastern United States. As a result, the dry simulation negated the effect that latent heating along the squall line had on the redistribution of PV. The result is impressive; the moist simulation (Fig. 2.10a) matches well with reanalysis data, which depicts a large dipole block in the north Atlantic. The dry simulation is entirely different (Fig. 2.10b). A very weak tropopause ridge appears just upstream of a strong upper-tropospheric low. The weak ridge building is the result of only weak high TPT (low PV) advection from the tropics without the aided support of diabatic PV redistribution. In the dry simulation, the decreased TPT (increased PV) that makes up the upper low southwest of the Azores is also the result of the absence of convection through the same process that failed to develop the blocking ridge.

The difference between moist and dry simulations for the January 2007 blocking case is less striking, but still very significant. These simulations were initialized at 1200 UTC 19 January, six hours prior to the heaviest precipitation during the rapid intensification of the cyclone over southeast Canada. At 96 hours into the simulation, the moist simulation depicts a very broad omega-block, with high TPT and a broad anticyclonic circulation extending as far as northern Greenland (Fig. 2.11a). 96 hours into the dry simulation shows a negatively tilted trough and ridge over the north Atlantic (Fig. 2.11b). In this simulation, advection of high TPT (low PV) from the tropics downstream from the strong upper trough has indeed resulted in the formation of a negatively tilted ridge. However, it is quite clear in comparing the two model simulations that the moist simulation is associated with a much higher amplitude anticyclonic circulation, as well as a pattern that looks much more like a block. In addition, the very high TPT (greater than 335 K) that was so prominent in the moist simulation is absent from the dry simulation.

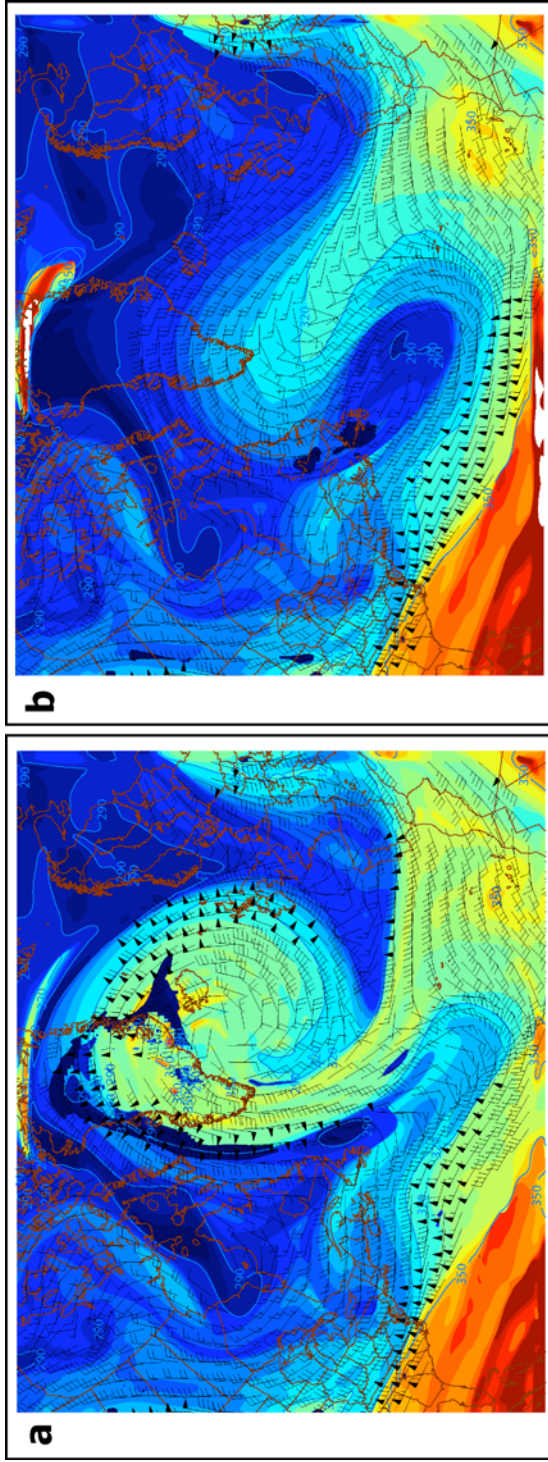


Figure 2.11. As in Fig. 10, but for forecast hour 96 of the January 2007 blocking case (1200 UTC 23 Jan).

Figure 2.12 compares the gradient of PV on the 315-325 K isentropic layer between the moist and dry simulations for the January 2007 blocking case at F12 and F60. At only 12 hours into the moist simulation (Fig. 2.12a), there is a considerable PV gradient, and thus a strong meridional wind, on the western flank of the developing ridge (positioned from New Brunswick south). This is in stark contrast to the dry simulation (Fig. 2.12b), which depicts only a weak PV gradient in the same region. In comparing the two simulations at F12, it is also important to note that other regions are *not* affected by diabatic heating. The strength of the PV gradient along the base of the trough south of Iceland is nearly identical in Figs. 2.12a and 2.12b. This further confirms the dramatic effects diabatic heating has had on the formation of the ridge in only 12 hours. By F60, the moist simulation depicts a highly amplified upper-tropospheric ridge (Fig. 2.12c) with a strong PV gradient from northeast Canada south to the base of the upper trough. Without the diabatically forced decrease in upper-tropospheric PV, the ridge has a much smaller amplitude and a far weaker PV gradient on the western side of the ridge (Fig. 2.12d).

At least in these simulations, it is likely that the redistribution of PV due to latent heating during rapid cyclogenesis resulted in increasing the PV gradient, and thus the strength of the upper jet, on the western flank of the developing ridge in both blocking cases. Thus, not only did latent heating contribute to producing the anomalously low PV (high TPT) within the blocking ridge, but it also likely increased the amount of advection of low PV (high TPT) from the tropics due to the increased upper-tropospheric PV (TPT) gradient.

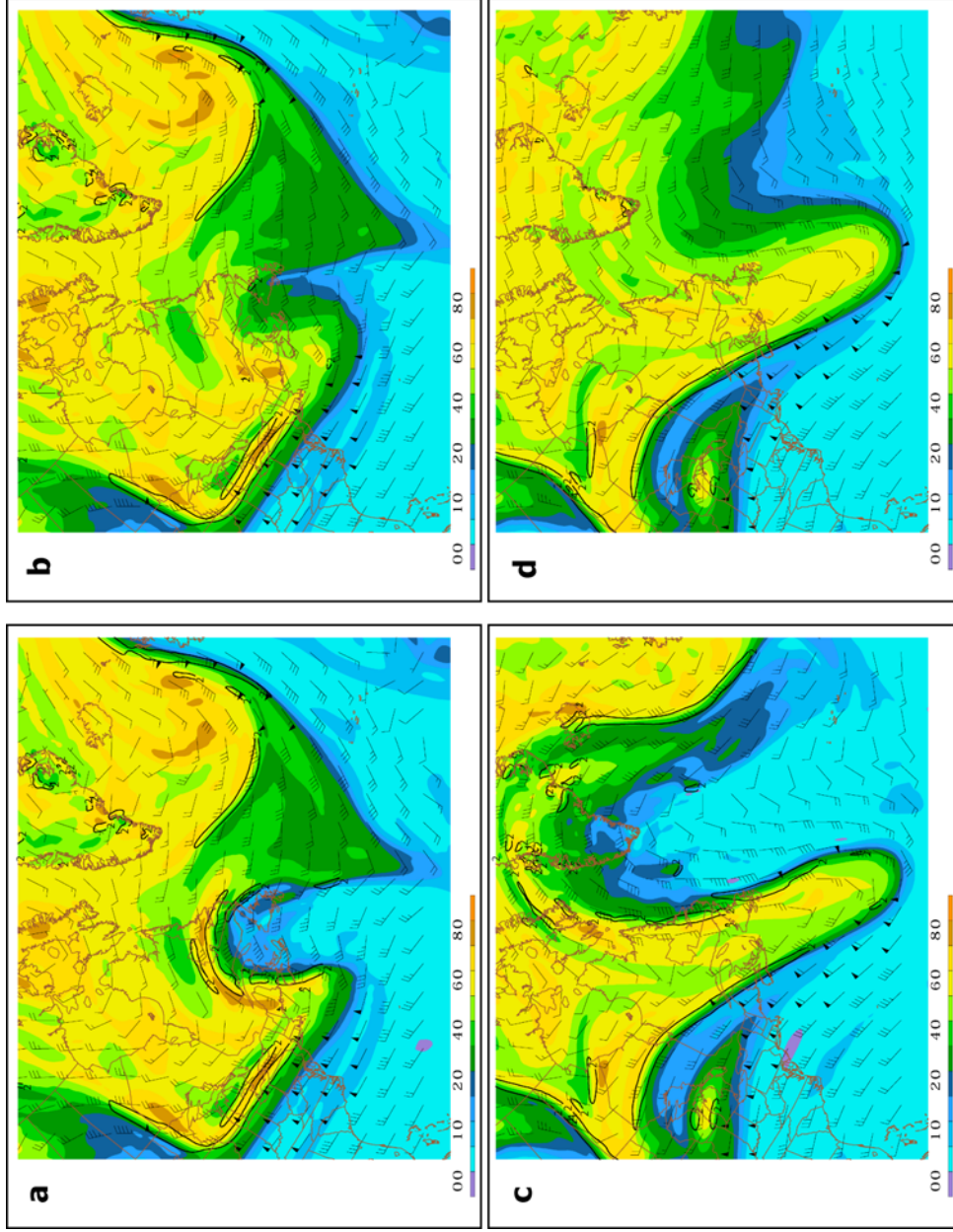


Figure 2.12. Ertel PV on the 315-325 K isentropic layer (colored fill) and magnitude of the PV gradient (contoured, interval 2×10^{-5} PVU m^{-1}) for (a) F12, moist simulation, (b) F12, dry simulation, (c) F60 moist simulation, and (d) F60, dry simulation.

2.5 Adjoint sensitivity study

a. Introduction

In this section, a set of adjoint sensitivity studies will be performed to assess the sensitivities of the PV within the simulated blocking anticyclone to the model forecast trajectory. The goal of a sensitivity study is to estimate how a particular differentiable function of the model forecast state (called a response function, R) of a numerical weather prediction (NWP) forecast defined at a specific forecast time (t_f) can be modified by changing the model initial (\mathbf{x}_0) or forecast state (\mathbf{x}_τ), prior to that final forecast time. This estimate, δR , is obtained by evaluating the inner product of a sensitivity gradient ($\partial R / \partial \mathbf{x}_\tau$, the gradient of R with respect to the model state at some forecast time, τ , $0 \leq \tau < t_f$) with a contemporaneous perturbation to the model state ($\delta \mathbf{x}_\tau$):

$$\delta R = \left\langle \frac{\partial R}{\partial \mathbf{x}_\tau}, \delta \mathbf{x}_\tau \right\rangle$$

The adjoint of an NWP model² is the most efficient means of calculating the required sensitivity gradient (Errico 1997). In principle, the results of an adjoint study can be used to determine how various perturbations to the model initial conditions would change the strength of the block. The adjoint model and the definitions of the response functions used are described below.

In order to identify specific regions and model state variables to which the development of the block is most sensitive, this study will define the response function as the

² Strictly speaking, the adjoint is defined for the tangent linear model (TLM, the nonlinear model linearized about a model forecast trajectory). For brevity, however, we will refer to the adjoint as the adjoint of the NWP model.

low PV within the blocking anticyclone at various forecast times. The Ertel PV in the MM5 sigma coordinate system is:

$$q = \frac{g}{p^*} \left(\left(\frac{\partial v}{\partial \sigma} \frac{\partial \theta}{\partial x} - \frac{\partial u}{\partial \sigma} \frac{\partial \theta}{\partial y} \right) - \frac{\partial \theta}{\partial \sigma} \left(f + \frac{\partial v}{\partial x} - \frac{\partial u}{\partial y} \right) \right)$$

Here, p^* is defined as the difference between surface pressure and the pressure at the top of the column.

b. Adjoint modeling system

The adjoint model used for this study is a component of the MM5 Adjoint Modeling System (Zou et al. 1997). This modeling system, based upon version one of the Pennsylvania State University/National Center for Atmospheric Research fifth generation mesoscale model (MM5), includes the nonlinear MM5 model, its tangent linear model (TLM), and corresponding adjoint. For all of the sensitivity calculations performed, the nonlinear version of the MM5 is used to create a basic state about which the TLM and adjoint models are linearized. For the TLM and adjoint integrations, the basic state is updated every time step. The adjoint code has been modified as described by Kleist and Morgan (2005) in order to eliminate the non-physical oscillation in the sensitivity gradients associated with the adjoint of the leapfrog time stepping scheme. This modification allows for an evaluation of the time evolution of the forecast sensitivities.

The domain for the nonlinear, TLM, and adjoint integrations is a 40 km, 200 x 160 horizontal grid (model domain is the same as the moist/dry simulations in Fig. 2.11), with 20 evenly spaced sigma levels in the vertical, and a top pressure level in the model of 100 hPa. The nonlinear model is initialized from the National Centers for Environmental Prediction

(NCEP) final analysis ($1^\circ \times 1^\circ$ global grid) interpolated to the MM5 grid, and lateral boundaries are updated using the NCEP final analyses. The nonlinear integrations use the following physical parameterizations: the Grell convective scheme, a bulk aerodynamic formulation of the planetary boundary layer, horizontal and vertical diffusion, dry convective adjustment, and explicit treatment of cloud water, rain, snow and ice. The TLM and adjoint integrations use the same parameterizations (or their adjoints), but the effects of moisture are neglected. This means that the TLM and adjoint models are integrated using only dry dynamics about the moist basic state created from the nonlinear model run. While one can obtain useful qualitative information from such a study, perturbations to the initial PV field would have to be made in order to assess that the results are quantitatively accurate.

Each sensitivity study begins at 1200 UTC 19 January 2007, six hours prior to the amplification of the initial ridge associated with the explosive cyclogenesis described in section 3. In order to identify those features to which the low values of upper-tropospheric PV within the block are most sensitive, three response functions were defined:

$$R_1 = \text{PV} < 0.00 \text{ PVU between } \sigma=0.15 \text{ and } \sigma=0.25 \text{ at 1200 UTC 20 January;}$$

$$R_2 = \text{PV} < 0.25 \text{ PVU between } \sigma=0.15 \text{ and } \sigma=0.25 \text{ at 1200 UTC 20 January.}$$

Thus, response functions R_1 and R_2 focus on the initial ridge building, and measure the low PV within the developing ridge. A third response function focuses on a more mature stage of block development and is defined at 48 h into a simulation ending at 1200 UTC 21 January:

$$R_3 = \text{PV} < 0.00 \text{ PVU between } \sigma=0.15 \text{ and } \sigma=0.25 \text{ at 1200 UTC 21 January.}$$

Figure 2.13 shows a superposition of the Ertel PV on the three sigma levels on which the response functions described above are defined. In comparing Fig. 2.13a (R_1) and Fig. 2.13b (R_2), the areal differences in R at forecast hours 24 (hereafter referred to as F24)

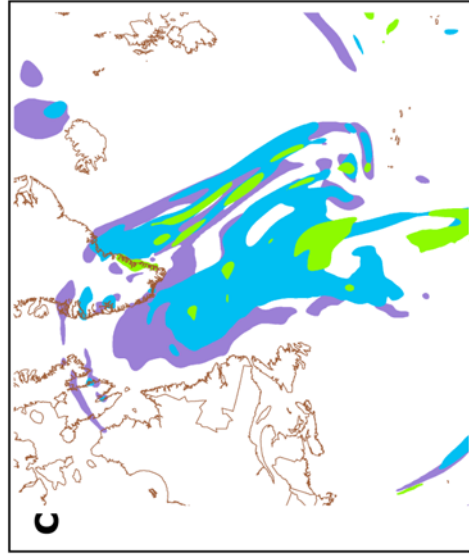
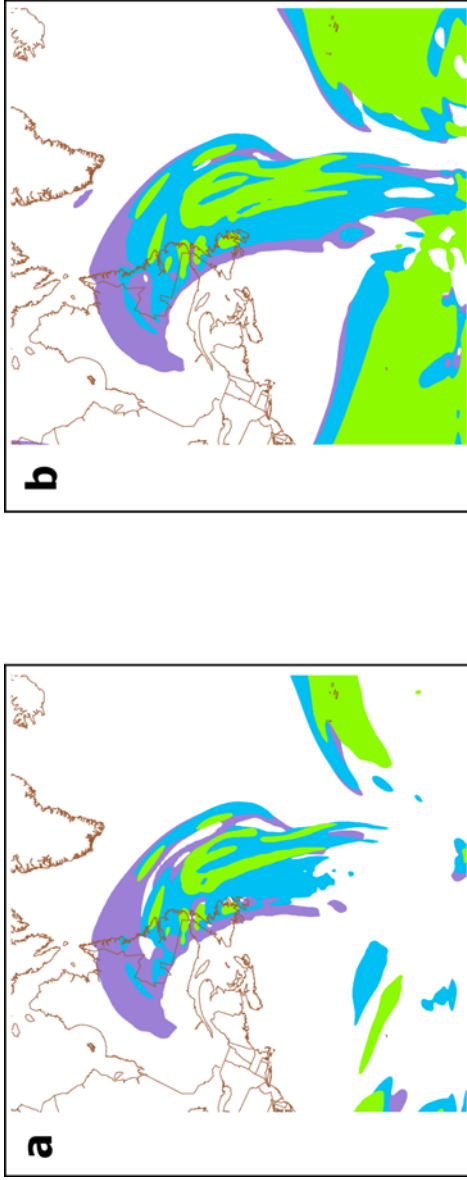


Figure 2.13. (a) Negative PV on the .15 σ -level (shaded, green), .20 σ -level (shaded, blue), and .25 σ -level (shaded, purple) for F24. (b) As in (a), except for PV less than 0.25 PVU. (c) As in (a), except for F48.

become clear. Because negative PV in the mid-latitude upper troposphere in the Northern Hemisphere is very anomalous, Fig. 2.13a depicts a response function with a smaller region than Fig. 2.13b. Thus, the sensitivities of R_1 will be associated with only the lowest PV within the developing block, and for R_2 , the sensitivities will essentially be associated with the full upper-tropospheric PV within the developing block. At F48, a large portion of the western flank of the ridge has $PV < 0$, so R_3 (Fig. 2.13c) has a slightly larger horizontal extent than R_1 .

c. Sensitivities of R_1 to vorticity

Figure 2.14a shows sensitivities of R_1 to vorticity at the $\sigma=0.175$ level at F6 (18 hours before the response function is defined), as well as absolute vorticity from the TLM at the same level. A region of large, positive sensitivities lies along the vorticity gradient along and off the coast of Maine, on the western flank of the amplifying ridge. The sensitivity field reveals that a negative perturbation to the vorticity field in this region would result in lower PV within the negative PV regions of the ridge 18 hours later. This local sensitivity maximum which is seen on several half-sigma levels throughout the upper troposphere (not shown), is collocated with a region where there has been a large amount of differential diabatic heating, and thus PV redistribution, as is seen on the dynamic tropopause in section 3 (Fig. 2.9d). Thus, the very low PV within the ridge 24 hours into the simulation is highly sensitive to latent heating (and thus, the *erosion* of upper-tropospheric PV) that occurs near the developing cyclone's center, as well as along the cold front.

In Fig. 2.14a, there is also a broad region of negative sensitivities to vorticity at $\sigma=0.175$ throughout a large portion of the upper trough at F6. Thus, raising the vorticity in

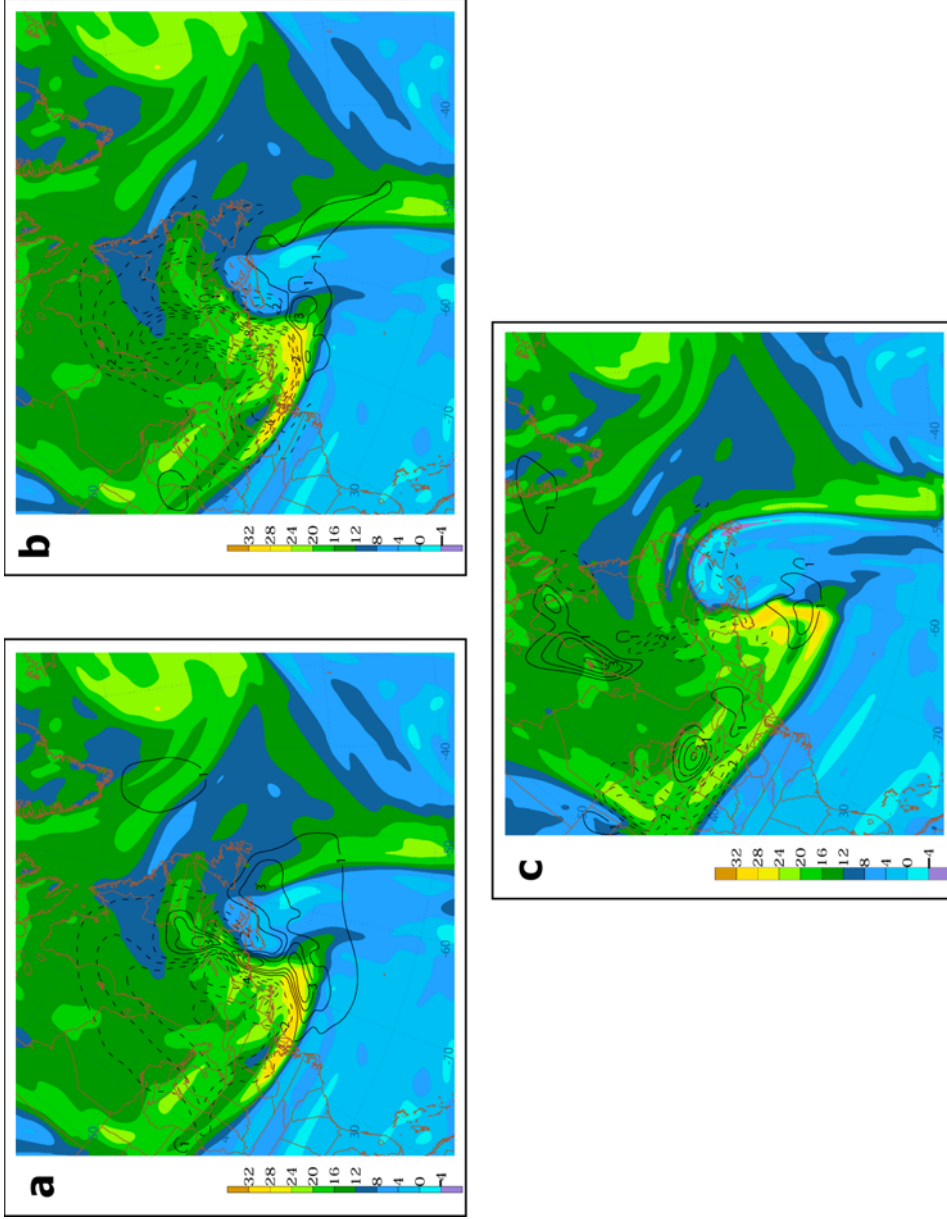


Figure 2.14. (a) $\sigma=0.175$ absolute vorticity (colored fill, interval 4 s^{-5}) and sensitivity of R_1 to absolute vorticity on the $0.175\text{-}\sigma$ surface (contours, interval 1 PVU s) at F6. (b) As in (a), but for R_2 . (c) As in (a), but for R_3 and at F12.

the upper trough will result in lowered PV within the ridge at the final time. There are two processes which provide a consistent explanation for this result. First, increased advection of low PV from the tropics due to a stronger upper-tropospheric cyclonic circulation upstream of the ridge would result in lower PV within the ridge 18 hours later. Second, a stronger upper-tropospheric trough would likely enhance positive vorticity advection by the thermal wind downstream, thus resulting in more ascent and stronger development of the cyclone. It is plausible, then, that a stronger trough at F6 creates stronger low PV-advecting winds into the ridge, as well as enhanced precipitation and latent heating during cyclogenesis.

d. Sensitivities of R_2 to vorticity

By defining the response function as $PV < 0.25$ PVU, the sensitivity fields will be associated with a larger portion of the ridge, rather than just the exceptionally small PV within the ridge. Figure 2.14b shows sensitivities of such PV to vorticity at $\sigma=0.175$ at F6. As opposed to Fig. 2.14a, where a maximum in sensitivities was located on the western flank of the developing ridge, the sensitivities of $PV < 0.25$ are predominantly negative throughout the upper trough and the western flank of the downstream ridge. This implies that by perturbing the vorticity field at F6 and thereby creating a stronger cyclonic circulation within the trough, the result would be stronger advection of low PV from the tropics into the developing ridge. Therefore, it is likely that the *negative* PV within the ridge at F24 is closely linked to latent heating, but that the air mass within the ridge where PV is uniformly between 0 and 0.25 PVU is largely advected into the ridge from the tropics. As previously discussed, prior blocking research (Illari 1984; Nakamura and Wallace 1993) has shown that the low PV found within blocking anticyclones is advected from the tropics. This analysis

shows that while advection may partially explain the development of the January 2007 blocking event, regions of very low PV within the blocking ridge appear to be created through latent heating.

e. Sensitivities of R_3 to vorticity

By F48 (1200 UTC 21 January 2007), the ridge has amplified to span over 30° latitude. The second shortwave, as described in section 2.3, has rounded the base of the trough and the secondary cyclogenesis event is underway southeast of Newfoundland. A new response function has been defined, which encapsulates the negative PV within the blocking ridge at F48 between $\sigma=0.15$ and 0.25 .

Figure 2.14c shows sensitivities of R_3 to vorticity at $\sigma=0.175$ at F12. In this scenario, there is a general absence of large magnitude sensitivities within the ridge and the upstream vorticity maximum. However, farther upstream, there is a region of negative sensitivities to vorticity. These sensitivities are collocated with absolute vorticity maxima imbedded within a shortwave. One vorticity maximum is located over Minnesota, and another is downstream, from northern Illinois to Ohio. Throughout the evolution of this adjoint simulation (not shown), the negative sensitivities generally remain coherent, and follow the absolute vorticity maxima within the “secondary shortwave,” which illustrates that the low PV within the developing block is sensitive to the strength of the shortwave that exists much further upstream. Specifically, an increase in the strength of the vortex would result in a stronger anticyclonic circulation within the downstream ridge 36 hours later. This process was shown to be integral in further amplification of the blocking ridge in an analysis of the case in section 2.3. This second shortwave residing over the western Great Lakes at F12 ultimately

led to a secondary cyclogenesis event over the northwest Atlantic. This contributed to PV redistribution associated with the diabatic heating, leading to an increase in anticyclonic circulation and further amplification of the ridge.

f. Discussion

The adjoint sensitivity study provides further evidence that the development of the January 2007 blocking event in the North Atlantic was assisted by latent heating during two major cyclogenesis events. That the upper-tropospheric sensitivity fields throughout each simulation discussed were generally confined to within the upstream upper trough suggests that the lowest PV within the developing block was not merely advected northward from lower latitudes. Rather, the sensitivities to upper-tropospheric vorticity appear to be located within one of two regions:

- 1) The sensitivities of the response function to vorticity are negative and located within upper-tropospheric vorticity maxima, implying that the strength of an upstream upper-tropospheric wave is crucial in the development of low PV within the downstream ridge.

- 2) The sensitivities of the response function to vorticity are positive and located on the western flank of the developing ridge, implying that the low PV within the block is sensitive to processes that result in a lowering of the upper-tropospheric vorticity just downstream of an upper-tropospheric trough, such as diabatic heating maximized in the middle troposphere.

It is of interest to note that adjoint sensitivities calculated with respect to other variables, including temperature and vertical motion, do not lend themselves to clear

interpretation. The sensitivity patterns, particularly in the lower and mid-troposphere (not shown) lack coherence, making their interpretation quite challenging.

2.6 Conclusion

Blocking of the mid-latitude westerlies has a major impact on the weather, as synoptic-scale systems are averted around a large, nearly stationary anticyclone. These issues, as well as difficulties associated with the predictability of block onset and duration make blocking an important phenomenon to fully understand. A number of studies (e.g., Konrad and Colucci 1988; Nakamura and Wallace 1993) have shown a strong correlation between block onset and rapid upstream cyclogenesis, which suggests that there may be a link between latent heating and block development. In this study, through the use of an adapted version of the blocking index developed by Pelly and Hoskins (2003), a catalog of North Atlantic blocking events from 2000-07 was created. It was acknowledged that some cases were associated with regions of anticyclonic circulations far removed from the mid-latitude westerlies, and thus non-blocking events. However, the majority of cases identified closely resembled classic blocking patterns.

In order to analyze the development of major blocking patterns, two events were chosen; one was taken from the list of events identified using the adapted index (Table 2.1), and another was a widely studied event from February 1983. Through an analysis of these cases of North Atlantic blocking, this study has shown that latent heating can act as a catalyst in the formation of a block. By employing various techniques, it has been shown that the anomalously low PV that makes up a blocking anticyclone can be at least partially traced back to latent heating upstream. In the case of the February 1983 blocking event, the

lowering of upper-tropospheric PV was a direct result of convective precipitation along a cold front over the southeast United States. In January 2007, synoptic-scale heavy precipitation fell during a rapid cyclogenesis event over southeastern Canada.

Through analysis of “fake dry” model simulations of each block, it was demonstrated that diabatic processes played an integral role in producing the low upper-tropospheric PV (high TPT) and high amplitude ridges in both cases. In the February 1983 case, the dry simulation completely failed to produce a large ridge over the North Atlantic. The dry simulation of the January 2007 blocking event yielded a strongly negatively tilted ridge, though of a much lesser amplitude than in the moist simulation.

The importance of latent heating in developing these two blocks was also shown using an adjoint sensitivity study. In the case of the January 2007 blocking episode, it was revealed that the negative upper-tropospheric PV within the developing ridge was highly sensitive to the strength of the upstream upper trough. Additionally, a region of high sensitivities to upper vorticity was located within a region where surface explosive cyclogenesis was taking place. That the cyclogenesis event was associated with large amounts of latent heating confirms the importance of diabatic heating in the creation of the lowest PV within the block. Given the scale of blocking anticyclones and the importance of diabatic heating suggested by the results presented in this work, future work should include the use of a global, full physics adjoint to more clearly elucidate those features to which the PV in the blocking anticyclone is most sensitive.

By rapidly decreasing the upper-tropospheric PV (increasing the TPT), latent heating can also drastically modify the PV *gradient* on the western flank of a developing ridge. Because cyclogenesis occurs upstream of an upper-tropospheric ridge axis, latent heating and

PV redistribution is favored on the western flank of a ridge. Not only does this process allow low upper-tropospheric PV to be ingested into the blocking ridge, it also increases the PV gradient aloft, creating much stronger winds advecting low PV from lower latitudes into the ridge. The poleward transport of anomalously low PV on the western side of a block was noted as a common occurrence by Mahlman (1979). This suggests that diabatic heating at the inflection point between a trough and downstream ridge may enhance the potential for a block to develop due to an increased PV gradient.

Additionally, blocking patterns are commonly formed through anticyclonic wave-breaking events, and the presence of anomalously low PV within the blocking ridge may account for some of this process. The rapid decrease of PV aloft results in further amplification of a ridge and an increase in the strength of the anticyclonic circulation. During the development of the February 1983 blocking event, the sudden appearance of low upper-tropospheric PV within the ridge assisted in forcing the ridge to break anticyclonically and cutting off the downstream trough. This process resulted in the formation of the dipole blocking structure, and may not have occurred without the presence of such anomalously low upper-tropospheric PV within the ridge.

It should be clearly stated that this research does not attempt to discount prior research on block development which focused on adiabatic processes. It is merely suggesting that some blocking events appear to develop solely due to diabatic anticyclogenesis, and others may simply be assisted by diabatic processes. Many adiabatic processes that have been noted to be necessary in block development can be enhanced by diabatic heating, such as the advection of low PV from low latitudes due to an increase in the

strength of the meridional jet, and the increase in strength of the anticyclonic circulation of a ridge, resulting in a wave-breaking event.

Acknowledgements. The data were provided by the Data Support Section of the Computational and Information Systems Laboratory at the National Center for Atmospheric Research. NCAR is supported by grants from the National Science Foundation.

Chapter 3. The influence of tropical cyclone outflow on the upper-tropospheric circulation

3.1 Introduction

The primary circulation attributed to a tropical cyclone (TC) is that of a warm-core vortex, where the strongest cyclonic circulation lies near the surface and gradually weakens with height. Above the cyclonic circulation is a broad anticyclone, which tends to have a length-scale larger than that of the lower-tropospheric cyclonic circulation. A TC's secondary circulation is an "in-up-out" circulation driven by latent heating, with the strongest ascent near the TC's center (i.e., eye-wall), and convergent (divergent) flow in the lower- (upper-) troposphere.

Throughout the lifetime of a TC, attention is primarily focused on the track and intensity of the TC's lower-tropospheric cyclonic circulation, as it is to this circulation that loss of life and property due to wind, storm surge, and inland flooding is directly attributed. From a PV perspective, this lower-tropospheric circulation is associated with a cyclonic PV tower that extends from just above the surface to the upper troposphere. This PV tower lies below a lens of anticyclonic PV in the upper troposphere (i.e., an elevated dynamic tropopause) that is a manifestation of PV redistribution associated with convective heating. This lens of locally anomalous anticyclonic PV defines the TC *outflow*. Situated in the divergent flow above the cyclonic PV tower, TC outflow tends to expand away from the TC's center during intensification (Rappin 2004). Wu and Kurihara (1996, hereafter WK) showed that after the TC's cyclonic PV anomaly weakens, the upper-tropospheric negative PV anomaly associated with the outflow often lingers for several days.

While attention is typically focused on the TC's potentially damaging cyclonic circulation, the evolution of TC outflow is also of practical importance for a number of reasons. Prior to the demise of the cyclonic circulation, the wind field attributed to the outflow can affect the vertical wind shear experienced by the TC; if the outflow is asymmetric with respect to the hurricane's center, vertical wind shear induced by the outflow's anticyclonic circulation will be stronger than if the outflow were symmetric with respect to the TC center. Similarly, upper-tropospheric winds associated with an asymmetric outflow can also alter the steering flow of the TC (WK).

An additional distinction between the lower tropospheric cyclonic circulation and the TC outflow is that the outflow has a spatial scale much larger than that of the hurricane's cyclonic circulation, and as a consequence, can have long-lasting effects (an outflow "footprint") on the upper-tropospheric large-scale circulation following the spin-down of the cyclonic circulation. This outflow footprint can be advected by the upper-tropospheric flow until gradual diabatic redistribution of PV (i.e., through radiative cooling) weakens the anomaly. Prior to the dissipation of the outflow PV anomaly, the height perturbations associated with it can be realized as substantial anomalies in the climatology of the subtropics and mid-latitudes. Hoskins et al. (1985) suggested that radiative cooling in the upper troposphere attenuates upper-tropospheric low PV anomalies on time scales of about a week. Furthermore, if the outflow from a TC extends to a mid-latitude PV gradient, downstream Rossby waves may be excited. If the outflow PV differs from that of the ambient upper-tropospheric PV, an outflow jet forms along the PV gradient.

This chapter will document the structure and evolution of TC outflow from Atlantic Hurricanes Ophelia and Rita (2005) and attempt to identify both hurricanes' outflow

“footprints” as well as their contribution to the upper-tropospheric circulation using analyzed data, observations, and numerical simulations. Particular attention will be placed on the excitation, by the outflow of Ophelia, of a Rossby wave train downstream that appears to have created a favorable environment for the development of Hurricane Rita. The data used are described in section 3.2, as well as an analysis of the case study. An outline for future work can be found in section 3.3.

3.2 Case study

a. Data

The analyzed data sets used in the following discussion are the National Centers for Environmental Prediction (NCEP) global tropospheric final analysis data, available from the National Center for Atmospheric Research Data Support Services as data set ds083.0.

b. Synoptic Overview

Hurricane Ophelia developed off the coast of southern Florida on 6 September 2005 and strengthened to category 1 hurricane status while moving northward along the southeast coast of the United States. By 1200 UTC 16 September (Fig. 3.1a), Ophelia had begun to weaken off the North Carolina coast. Ophelia’s outflow, as seen on the dynamic tropopause as an expansive region with tropopause potential temperature (hereafter, TPT) exceeding about 350 K, encompassed an area extending northeastward from the northeast Gulf of Mexico to Halifax, Nova Scotia, and from the Ohio Valley to just east of Bermuda. At this time, the cyclonic portion of Hurricane Ophelia was depicted as a small area (approximately 300 km in diameter) of high lower-tropospheric PV off of the North Carolina coast. A

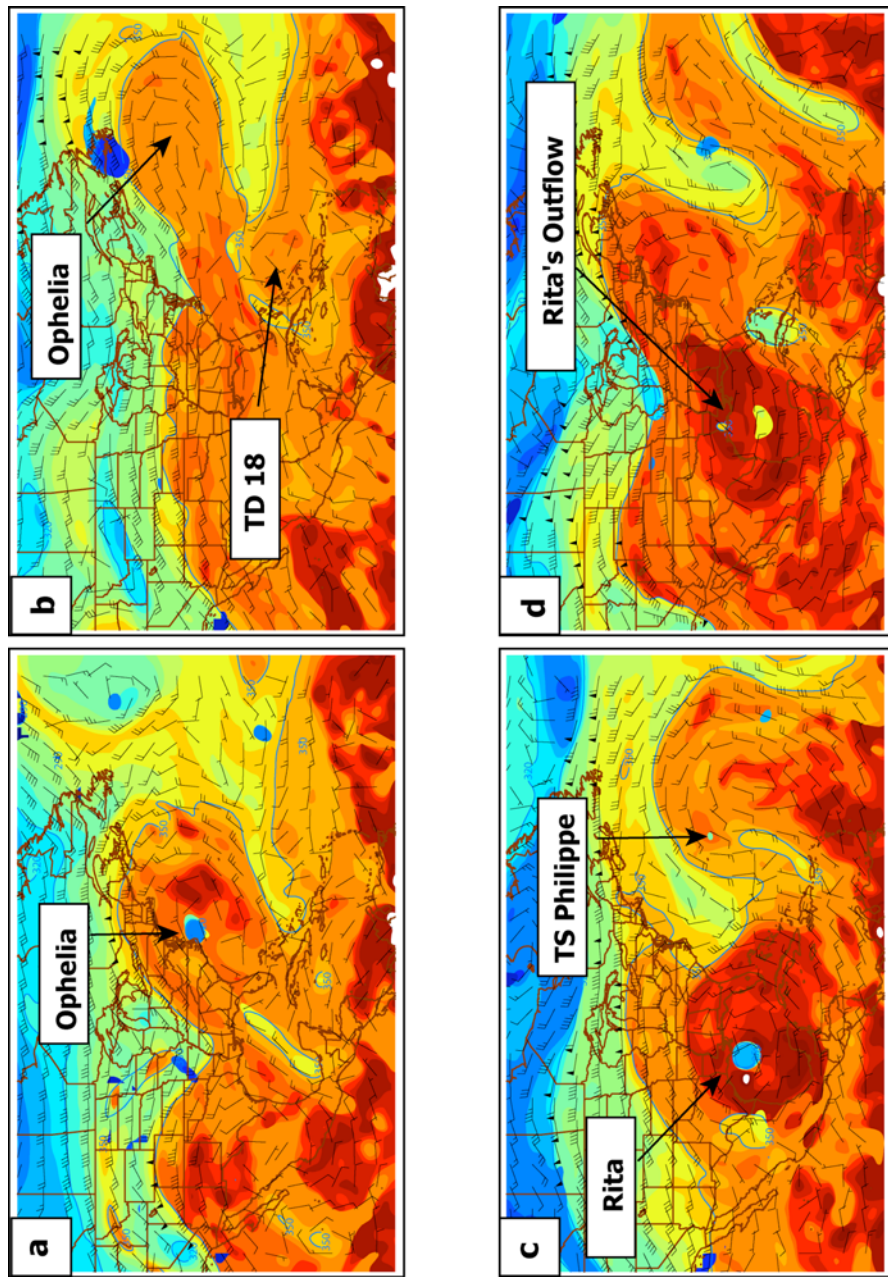


Figure 3.1. Potential temperature on the dynamic tropopause (color filled, interval 5 K) and wind (ms⁻¹) for (a) 1200 UTC 16 September 2005; (b) 1800 UTC 18 September; (c) 1200 UTC 23 September, and (d) 1800 UTC 26 September.

smaller area of TPT exceeding 370 K was also positioned to the east of the hurricane. Downstream from the large outflow-induced anticyclonic circulation was a weak, anticyclonically breaking trough, extending east-northeast from the Bahamas.

By 1800 UTC 18 September (Fig. 3.1b), Hurricane Ophelia had already transitioned into an extratropical storm, leaving behind a broad, elliptical upper-tropospheric anticyclonic circulation over the northwest Atlantic. This circulation could be tracked for several days until it gradually weakened. The transitioned cyclone was manifest on the tropopause map as an area of lower tropospheric PV exceeding 1.5 PVU located to the south of Newfoundland under strong shear along the tropopause. Meanwhile, a portion of the anticyclonically breaking trough had become cut off and was located over the Bahamas. Positioned in a favorable location for ascent downstream from this cut-off upper wave was Tropical Depression 18, which would later become a devastating category 5 storm, Hurricane Rita. On the dynamic tropopause, evidence for the nascent tropical storm was a region of locally high TPT north of Hispaniola.

At 1200 UTC 23 September (Fig. 3.1c), Hurricane Rita was a category 4 hurricane with its center positioned approximately 300 km south of the Louisiana coast. Unlike Hurricane Ophelia at its maximum intensity, Rita's outflow was associated with a very broad region (nearly 2500 km at its greatest diameter) of TPT over 370 K. Downstream of the outflow was an upper trough off the east coast of the United States. As had occurred with Hurricane Ophelia's outflow, the outflow of Hurricane Rita broke anticyclonically north of the upper trough, which eventually became cut off by the northeastwardly expanding anticyclonic circulations associated with both Hurricanes Rita and Philippe (the latter located

in the northwest Atlantic, also seen on the dynamic tropopause as a broad region of anticyclonic circulation).

As illustrated by WK, when the region of anomalously low PV associated with the outflow nears a mid-latitude upper-tropospheric jet, it becomes stretched along the axis of the jet. This scenario occurred with Hurricane Rita's outflow after the hurricane made landfall and weakened over the south central United States. This southwest-northeast tilt of the outflow "footprint" can be seen at 1800 UTC 26 September (Fig. 3.1d). Two days after Hurricane Rita made landfall and weakened, the broad region of anomalously high TPT (370 K) which was once associated with Rita's outflow remained over the southern United States and western Gulf of Mexico. Another piece of this circulation had been advected northeastward toward eastern Canada. Over time, the area of relatively high TPT over the southern United States was gradually advected westward into the eastern Pacific, and eventually cooled diabatically (not shown).

The upper-tropospheric circulation in Fig. 3.1d also illustrates how the outflow "footprint" left over from TCs can dramatically alter the circulation of the tropics and subtropics. From animations of the dynamic tropopause (not shown), it appears that the outflows from Hurricanes Rita and Philippe contributed to the amplification of downstream Rossby waves, ultimately causing the upper-tropospheric circulation to be more meridional.

A time-height cross-section of PV and relative humidity from Shreveport, LA is shown in Fig. 3.2. At approximately 0000 UTC 23 September, the PV in the 125-300 hPa layer decreased sharply, while the relative humidity in the layer increased to near saturation. This time corresponds with the passage of the "outflow front" on the dynamic tropopause over Shreveport (Fig. 3.1c). The front is also characterized by a shift to stronger southerly

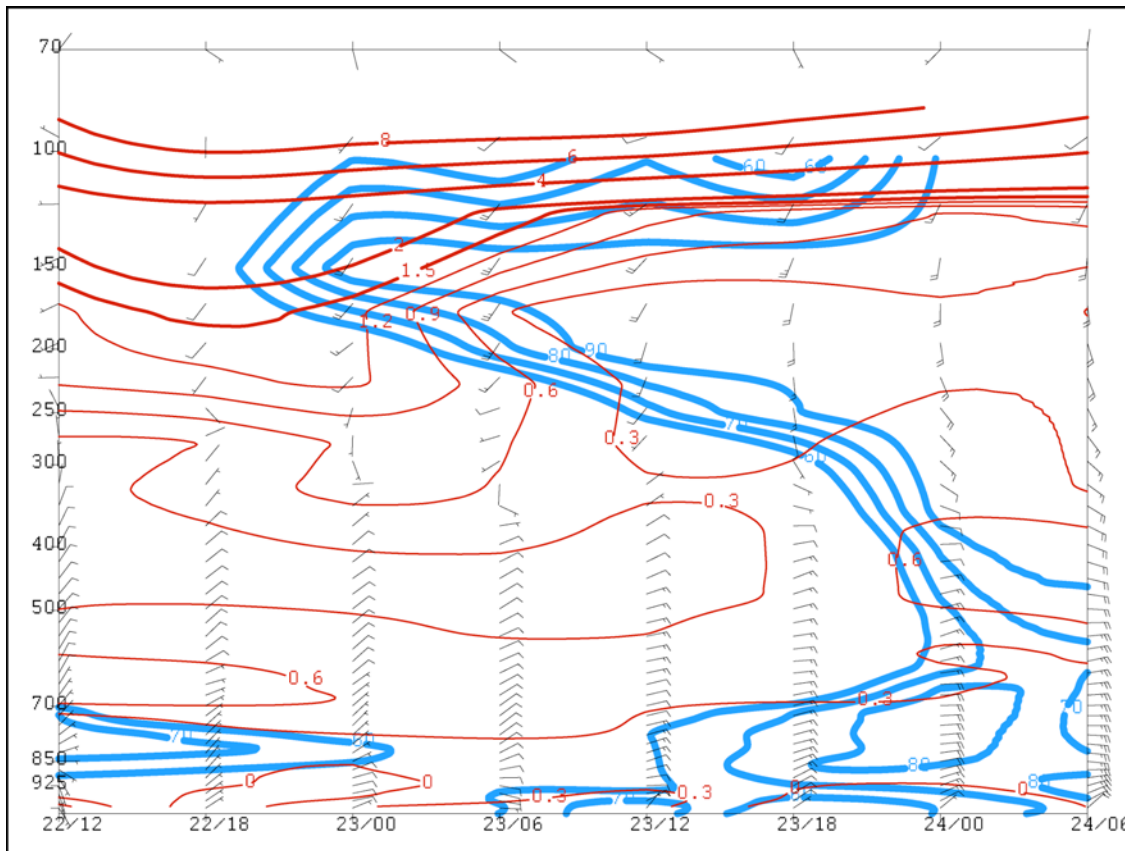


Figure 3.2. Time-height section of PV (red contours, PVU) and relative humidity (blue contours) for Shreveport, LA (KSHV) from 1200 UTC 22 September 2005 through 0600 UTC 24 September 2005.

winds within the outflow. The “lens” of low PV characterizing the outflow extends over a depth spanning from about 300 hPa to 125 hPa. The air within the outflow of a TC has its origins in the lower troposphere within the boundary layer. This is evident by the high (equivalent) potential temperature the air has on arrival at the tropopause as it spreads out (Figs. 3.1a, c, and d). The high equivalent potential temperature exists because of the near saturation of the lower tropospheric air at high temperature and low pressure near the cyclone center.

3.3 Discussion and future work

Latent heating in a TC increases TPT, and by extension, builds an upper-tropospheric anticyclone. Unlike blocking anticyclones of higher latitudes, the broad anticyclones that are associated with TC outflow are not necessarily stationary and these anticyclones cannot be explained adequately using adiabatic, advective dynamics. The outflow anticyclones that are most stationary are those located in the deep tropics, far removed from the prevailing westerlies of higher latitudes (e.g., Rita’s outflow). It is these anticyclones that can have the most significant seasonal climatological footprint. Those anticyclones that interact with the westerlies will have shorter lifespans – particularly if they are strongly strained by the ambient flow (e.g., Ophelia’s outflow).

Once the primary cyclonic circulation of the TC is no longer active, there is no mechanism to maintain the anticyclone. This is in direct contrast to a blocking anticyclone, which is able to advect PV from lower latitudes and maintain itself. The TC outflow anticyclone is an isolated vortex characterized by some of the *highest* TPT in the hemisphere within which it resides. Thus, advection of lower PV values into the anticyclone is

impossible. The longevity of an isolated TPT maximum is governed by the rate at which radiative cooling can erode the maximum.

In order to further characterize and define TC outflow, a set of numerical simulations of Hurricane Rita may be run: a control, “full physics” simulation and a “fake dry” simulation. This will allow a comparison of differences of the upper-tropospheric circulation with and without the hurricane’s outflow to take place. As in Shi et al. (1990), the simulations will also allow for the creation of trajectory analyses, in order to identify the full horizontal and vertical extent of the outflow, and evaluate the Lagrangian tendencies of PV in the outflow layer following the demise of the lower tropospheric cyclonic circulation. Additionally, using piecewise PV inversion, the magnitude of geopotential height perturbations attributed to the outflow’s anomalously low PV can be quantified.

Chapter 4. Conclusions

The conservation of potential vorticity (PV) in adiabatic, inviscid flow allows for PV anomalies created through latent heating to persist for several days after their creation. Chapter 2 of this study has shown the importance of diabatic heating in the formation of two cases of North Atlantic blocking. One event was a major high-amplitude blocking event from February 1983, and another event from January 2007 was identified through the use of a blocking index adapted from Pelly and Hoskins (2003). Blocking anticyclones in the Northern Hemisphere are associated with a broad region of anomalously low upper-tropospheric PV. Though most studies have attributed the existence and maintenance of such low PV at high latitudes to the poleward advection of low PV from the tropics, this study has shown that a potentially important contribution to the low PV within a block arises from diabatic heating in association with the precipitation distribution within an upstream cyclone. A few days prior to block onset in both cases, major cyclogenesis events (and for the February 1983 case, a strong cold front) over eastern North America resulted in a Lagrangian decrease in upper-tropospheric PV. This decrease in PV, coupled with strong advection from the tropics downstream of a large upper trough, helped to amplify the pre-blocking ridge.

By turning off the effects of latent heating in model simulations of each block, it was demonstrated that diabatic processes played an integral role in producing the low upper-tropospheric PV (high TPT) and high amplitude ridges in both cases. Similar results were shown using an adjoint sensitivity study. By defining a response function as the low upper-tropospheric PV within the blocking anticyclone at some forecast time, one can identify features that are significant in the block's development. In the case of the January 2007 blocking episode, it was revealed that the negative upper-tropospheric PV within the

developing ridge was highly sensitive to the strength of the upstream upper trough. Additionally, a region of high sensitivities to upper vorticity was located within a region where explosive surface cyclogenesis was taking place, thus further confirming the importance of diabatic heating in the creation of the lowest PV within the block.

Not only does latent heating aid in the production of a block through PV redistribution, but a rapid increase in TPT on the western flank of a ridge also has the effect of increasing the advection of low PV from lower latitudes by increasing the PV (TPT) gradient. In a future study, this enhanced advection and its role in blocking formation may be analyzed quantitatively using “PV surgery” (e.g., adjusting the diabatically altered PV on the western flank of the ridge to a more climatological value and re-running the model simulation with altered PV) or by simply comparing the magnitude of the jet in a moist and dry simulations.

As described in many previous studies on block research, a significant fraction of the low PV within a block is advected into the block from lower latitudes, downstream of an upper-tropospheric trough. Indeed, idealized numerical simulations of atmospheric flow produce blocking-like features with no latent heating at all. This study has shown that some of the PV in two cases of blocking originated from diabatic PV redistribution upstream from the block. Because it has been shown that the *lowest* (often negative) upper-tropospheric PV within the block can be traced back to diabatic processes, it is quite possible that the presence of such low PV in the upper troposphere assists in further amplification (and anticyclonic breaking) of the downstream ridge, thus eventually forming a block. Numerical simulations of the January 2007 block showed that, without latent heating, a negatively tilted ridge still is

able to develop, but it lacks the amplitude and classic omega-block shape shown in the moist simulation.

Through PV redistribution, latent heating occurring in a tropical cyclone (TC) also has a large impact on the flow in the upper troposphere. A large anticyclonic circulation with uniformly low PV (the outflow of the TC) lies above the TC's cyclonic circulation. The length-scale of the outflow is directly related to the strength of the TC, though its circulation can extend radially much farther than the cyclonic circulation at the surface. The eventual decay of the outflow circulation occurs long after the TC has made landfall. If the outflow circulation interacts with a mid-latitude jet, downstream Rossby waves can be excited. This can potentially increase shear in the subtropics, or as the case may have been in September 2005, assist in the development of additional tropical systems. Unlike mid-latitude blocks, these outflow anticyclones are not maintained by eddy fluxes of PV and can be strained into filaments by the ambient flow if they extend too far north into the westerlies.

References

- Alberta, T. L., S. J. Colucci, and J. C. Davenport, 1991: Rapid 500-mb cyclogenesis and anticyclogenesis. *Mon. Wea. Rev.*, **119**, 1186–1204.
- Barriopedro, D., R. García-Herrera, A. R. Lupo, and E. Hernández, 2006: A climatology of Northern Hemisphere blocking. *J. Climate*, **19**, 1042–1063.
- Berrisford, P., B. J. Hoskins, and E. Tyrlis, 2007: Blocking and Rossby wave breaking on the dynamical tropopause in the Southern Hemisphere. *J. Atmos. Sci.*, **64**, 2881–2898.
- Black, R. X., and R. M. Dole, 1993: The dynamics of large-scale cyclogenesis over the North Pacific Ocean. *J. Atmos. Sci.*, **50**, 421–442.
- Blackmon, M. L., 1976: A climatological spectral Study of the 500 mb geopotential height of the Northern Hemisphere. *J. Atmos. Sci.*, **33**, 1607–1623.
- _____, J. M. Wallace, N. C. Lau, and S. L. Mullen, 1977: An observational study of the Northern Hemisphere wintertime circulation. *J. Atmos. Sci.*, **34**, 1040–1053.
- Charney, J. G., and J. G. DeVore, 1979: Multiple flow equilibria in the atmosphere and blocking. *J. Atmos. Sci.*, **36**, 1205–1216.
- Colucci, S. J., 2001: Planetary-scale preconditioning for the onset of blocking. *J. Atmos. Sci.*, **58**, 933–942.
- Crum, F. X., and D. F. Stevens, 1988: A case study of atmospheric blocking using isentropic analysis. *Mon. Wea. Rev.*, **116**, 223–241.
- Derome, J., and A. Wiin-Nielsen, 1971: The response of a middle-latitude model atmosphere to forcing by topography and stationary heat sources. *Mon. Wea. Rev.*, **99**, 564–576.
- Dole, R. M., and N. D. Gordon, 1983: Persistent anomalies of the extratropical Northern Hemisphere wintertime circulation: geographical distribution and regional persistence characteristics. *Mon. Wea. Rev.*, **111**, 1567–1586.
- Dong, L., and S. J. Colucci, 2005: The role of deformation and potential vorticity in Southern Hemisphere blocking onsets. *J. Atmos. Sci.*, **62**, 4043–4056.
- Elliott, R. D., and T. B. Smith, 1949: A study of the effects of large blocking highs on the general circulation in the Northern-Hemisphere westerlies, *J. Meteor.*, **2**, 67–85.

- Errico, R. M., and T. Vukicevic, 1992: Sensitivity analysis using an adjoint of the PSU-NCAR mesoscale model. *Mon. Wea. Rev.*, **120**, 1644–1660.
- _____, 1997: What is an adjoint model? *Bull. Amer. Meteor. Soc.*, **78**, 2577–2591.
- Grell, G. A., J. Dudhia, and D. R. Stauffer, 1995: A description of the fifth-generation Penn State/NCAR Mesoscale Model. NCAR Technical Note, 122 pp.
- Hansen, A. R., and A. Sutera, 1995: The role of topography in the low-frequency variability of the large-scale midlatitude circulation. *J. Atmos. Sci.*, **52**, 2497–2508.
- Hoskins, B., M. McIntyre, and W. Robertson, 1985: On the use and significance of isentropic potential vorticity maps. *Quart. J. Roy. Meteor. Soc.*, **111**, 877–946.
- Illari, L., 1984: A diagnostic study of the potential vorticity in a warm blocking anticyclone. *J. Atmos. Sci.*, **41**, 3518–3526.
- Keller, L. M., M. C. Morgan, D. D. Houghton, and R. A. Lazear, 2006: Synoptic–dynamic climatology of large-scale cyclones in the North Pacific. *Mon. Wea. Rev.*, **134**, 3567–3587.
- Kleist, D. T., and M. C. Morgan, 2005: Interpretation of the structure and evolution of adjoint-derived forecast sensitivity gradients. *Mon. Wea. Rev.*, **133**, 466–484.
- Konrad, C. E., and S. J. Colucci, 1988: Synoptic climatology of 500 mb circulation changes during explosive cyclogenesis. *Mon. Wea. Rev.*, **116**, 1431–1443.
- Lackmann, G. M., L. F. Bosart, and D. Keyser, 1996: Planetary- and synoptic-scale characteristics of explosive wintertime cyclogenesis over the western North Atlantic Ocean. *Mon. Wea. Rev.*, **124**, 2672–2702.
- Lejenäs, H., and H. Økland, 1983: Characteristics of Northern Hemisphere blocking as determined from a long time series of observational data. *Tellus* **35A**, 350–362.
- Lin, B.D., 1982: The behavior of winter stationary planetary waves forced by topography and diabatic heating. *J. Atmos. Sci.*, **39**, 1206–1226.
- Lupo, A. R., and P. J. Smith, 1998: The interactions between a midlatitude blocking anticyclone and synoptic-scale cyclones that occurred during the summer season. *Mon. Wea. Rev.*, **126**, 502–515.
- Mak, M., 1991: Dynamics of an atmospheric blocking as deduced from its local energetics. *Quart. J. Roy. Meteor. Soc.*, **117**, 477–493.

- Mahlman, J. D., 1979: Structure and interpretation of blocking anticyclones as simulated in a GFDL general circulation model. *Proceedings of the 13th Stanstead Seminar*, Dept. of Meteorology, McGill University, Publ. in Meteor. No. 123.
- Merrill, R. T., 1993: Tropical cyclone structure, Chapter 2, *Global guide to tropical cyclone forecasting*. WMO/TC-No. 560, Report No. TCP-31, World Meteorological Organization; Geneva, Switzerland.
- Morgan, M. C., P. Neilley, and R. Dole, 1991: Scale interactions and diabatic processes during the development of an Atlantic blocking event. Preprints, *First Int. Symp. On Winter Storms*, New Orleans, LA, Amer. Meteor. Soc., 62-65.
- _____, and J. W. Nielsen-Gammon, 1998: Using tropopause maps to diagnose midlatitude weather systems. *Mon. Wea. Rev.*, **126**, 2555–2579.
- Namias, J. and P. F. Clapp, 1944: Studies of the motion and development of long waves in the westerlies, *J. Meteor.*, **1**, 57-77.
- Nakamura, H., and J. M. Wallace, 1990: Observed changes in baroclinic wave activity during the life cycles of low-frequency circulation anomalies. *J. Atmos. Sci.*, **47**, 1100–1116.
- _____, and J. M. Wallace, 1993: Synoptic behavior of baroclinic eddies during the blocking onset. *Mon. Wea. Rev.*, **121**, 1892–1903.
- _____, M. Nakamura, and J. L. Anderson, 1997: The role of high- and low-frequency dynamics in blocking formation. *Mon. Wea. Rev.*, **125**, 2074–2093.
- Pelly, J. L., and B. J. Hoskins, 2003: A new perspective on blocking. *J. Atmos. Sci.*, **60**, 743-755
- _____, and B. J. Hoskins, 2003b: How well does the ECMWF Ensemble Prediction System predict blocking? *Quart. J. Roy. Meteor. Soc.*, **129**, 1683–1702.
- Petterssen, S., 1956: *Weather Analysis and Forecasting, Vol. I*, McGraw-Hill, 428 pp.
- Quiroz, R. S., 1984: The climate of the 1983-84 winter—A season of strong blocking and severe cold in North America. *Mon. Wea. Rev.*, **112**, 1894-1912.
- Rappin, E., 2004: The role of environmental inertial stability on tropical cyclone intensification. M.S. thesis, Dept. of Atmospheric and Oceanic Sciences, University of Wisconsin-Madison.
- Reed, R. J., M. D. Albright, A. J. Sammons, and P. Undén, 1988: The role of latent heat release in explosive cyclogenesis: Three examples based on ECMWF operational forecasts. *Wea. Forecasting*, **3**, 217–229.

- Rex, D. F., 1950: Blocking action in the middle troposphere and its effect upon regional climate (II). The climatology of blocking action. *Tellus* **2**, 275-301.
- _____, 1951: Blocking action in the middle troposphere and its effect upon regional climate (I). An aerological study of blocking action. *Tellus* **3**, 196-211.
- Sanders, F., and J. R. Gyakum, 1980: Synoptic-dynamic climatology of the “bomb”. *Mon. Wea. Rev.*, **108**, 1589–1606.
- Schwierz, C., 2001: Interactions of Greenland-scale orography and extra-tropical synoptic-scale flow. Ph.D. dissertation, Swiss Federal Institute of Technology, 155 pp.
- _____, M. Croci-Maspoli, and H. C. Davies, 2004: Perspicacious indicators of atmospheric blocking. *Geophys. Research Letters*, **31**, L06125, doi:10.1029/2003GL019341
- Shi, J-J., S. W-J. Chang, and S. Raman, 1990: A numerical study of the outflow layer of tropical cyclones. *Mon. Wea. Rev.*, **118**, 2042-2055.
- Shutts, G. J., 1983: The propagation of eddies in diffluent jetstreams: Eddy vorticity forcing of blocking flow fields. *Quart. J. Roy. Meteor. Soc.*, **109**, 737-761.
- _____, 1986: A case-study of eddy forcing during an Atlantic blocking episode. *Adv. Geophys.*, **29**, 135-162.
- Simmons, A. J., J. M. Wallace, and G. W. Branstator, 1983: Barotropic wave propagation and instability, and atmospheric teleconnection patterns. *J. Atmos. Sci.*, **40**, 1363–1392.
- Tibaldi, S., and F. Molteni, 1990: On the operational predictability of blocking. *Tellus* **42A**, 343-365.
- Tracton, M. S., 1990: Predictability and its relationship to scale interaction processes in blocking. *Mon. Wea. Rev.*, **118**, 1666–1695.
- Walker, G. T., and E. W. Bliss, 1932: World Weather V. *Mem. Roy. Meteor. Soc.*, **4**, 53-84.
- Wallace, J. M., and D. S. Gutzler, 1981: Teleconnections in the geopotential height field during the Northern Hemisphere winter. *Mon. Wea. Rev.*, **109**, 784-812.
- Wiedenmann, J. M., A. R. Lupo, I. I. Mokhov, and E. A. Tikhonova, 2002: The climatology of blocking anticyclones for the Northern and Southern Hemispheres: Block intensity as a diagnostic. *J. Climate*, **15**, 3459–3473.

- Woollings, T. J., B. J. Hoskins, M. Blackburn, and P. Berrisford, 2008: A new Rossby wave-breaking interpretation of the North Atlantic Oscillation, *In Press*.
- Wu, C-C., and Y. Kurihara, 1996: A numerical study of the feedback mechanisms of hurricane-environment interaction on hurricane movement from the potential vorticity perspective. *J. Atmos. Sci.*, **53**, 2264-2282.
- Zou, X., F. Vandenberghe, M. Pondeva, and Y. H. Kuo, 1997: Introduction to adjoint techniques and the MM5 adjoint modeling system. NCAR Tech. Note NCAR/TN-435+STR, 110 pp. [Available from NCAR, P.O. Box 3000, Boulder, CO 80307-3000.]